174

SC-4440(RR)

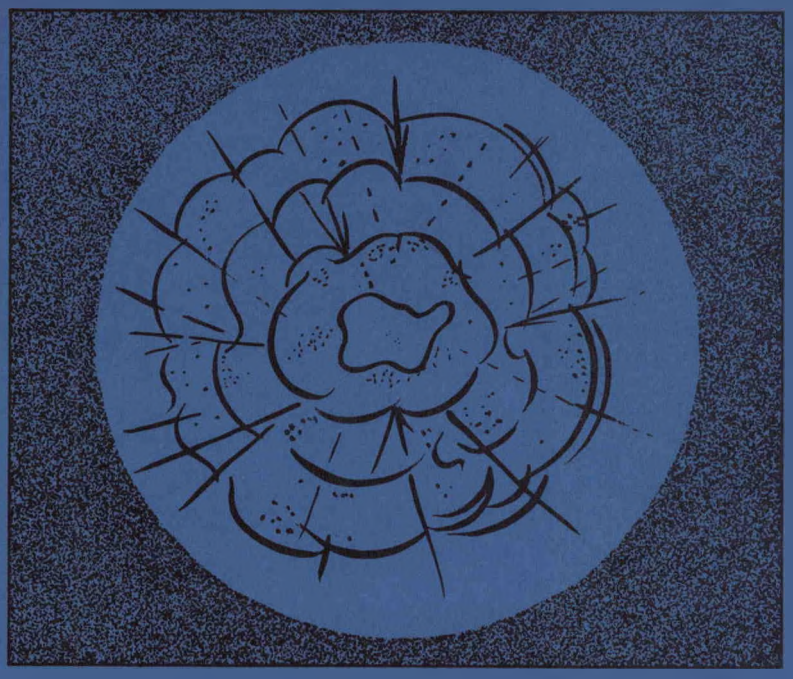

U.S. ATOMIC ENERGY COMMISSION
Albuquerque Operations Office
and
University of California
Lawrence Radiation Laboratory

FINAL REPORT

Project

COWBOY

Winnfield, Louisiana

DECEMBER 1959 - MARCH 1960

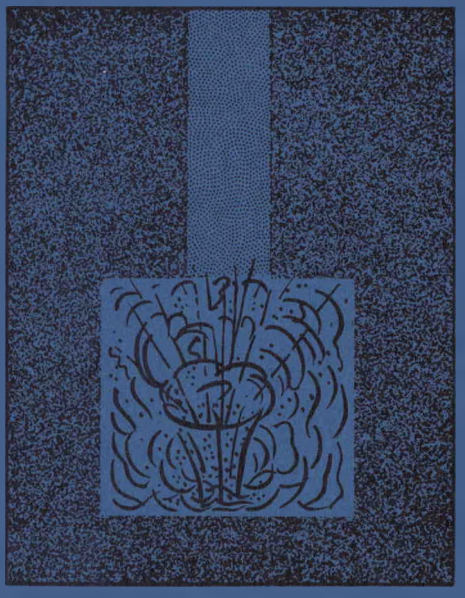

PARTICLE MOTIONS NEAR EXPLOSIONS IN HALITE

B. F. Murphey, 5112

June 1960
Sandia Corporation
Contractor for U. S. Atomic Energy Commission

SUMMARY OF SHOT DATA - PROJECT COWBOY

Shot no.	Date	Time (CST)	Yield (lbs)	Station	Type
1	17 Dec	0015	20	1.2	Coupled, 45-ft hole
2	17 Dec	0045	20	1.1	Decoupled, 12-ft dia. sphere
3	19 Dec	0000	100	1.1	Decoupled, 12-ft dia. sphere
4	19 Dec	0015	100	1.3	Coupled, 45-ft hole
5	23 Jan	0000:00.113	198.35	2.1	Decoupled, 30-ft dia. sphere
6	30 Jan	0001:00.112	200.0	2.1	Decoupled, 30-ft dia. sphere
7	30 Jan	0101:00.112	199.65	2.2	Coupled, 110-ft hole
8	6 Feb	0001:00.115	477.4	2.1	Decoupled, 30-ft dia. sphere
9	6 Feb	0101:00.113	499.7	2.3	Coupled, 110-ft hole
10	13 Feb	1901:00.113	954.0	2.1	Decoupled, 30-ft dia. sphere
11	13 Feb	2001:00.114	1003.0	2.4	Coupled, 110-ft hole
12	20 Feb	0001:00.112	929.0	1.1	Decoupled, 12-ft dia. sphere
13	20 Feb	0100:59.614	987.6	2.5	Coupled, 110-ft hole
14	27 Feb	0001:00.127	1902.4	1.1	Decoupled, 12-ft dia. sphere
15	28 Feb	0401:00.131	936.2	2.6	Coupled, 110-ft hole
16	3 Mar	2301:00.128	199.5	1.4	Coupled, 45-ft hole
17	4 Mar	0001:00.130	199.8	1.3-1	Coupled, 45-ft hole

Note: (1) All times for shots 5 through 17 are derived from comparisons with WWV. Accuracies are ± 0.001 sec, except for shot 15, which is ± 0.003 sec.

(2) All yields include "Nitramon" booster and detonator weights of either 2 or 3 pounds.

PARTICLE MOTIONS NEAR EXPLOSIONS IN HALITE

by

B. F. Murphey, 5112

June 1960

ABSTRACT

Comparative peak particle velocities and peak displacements were measured for tamped (coupled) and decoupled (by a cavity) explosions of high explosive in halite. Recordings are illustrated of particle velocity versus time in the salt medium and of pressure versus time on the cavity wall. Peak particle velocities from tamped shots decrease in amplitude as distance$^{-1.65}$ over distances equivalent to 40 to 800 feet for 1000 pounds high explosive. Permanent displacements in the region of observation were 0.01 inch or less and were, therefore, not accurately observable with available measuring apparatus.

Decoupling factors observed directly apply only to close-in stations. One method of extrapolating close-in data to compute distant decoupling factors gives numbers ranging from 40 to 100 for these particular experiments. Extrapolation to nuclear explosions still requires calculation or experiment and is not attempted here.

ACKNOWLEDGMENTS

Sandia Corporation measurements at Project Cowboy, Winnfield, Louisiana, were carried out under the general supervision of A. Dean Thornbrough. Ed S. Ames and Hervey L. Hawk were responsible for the successful operation of the instrumentation system. All three have contributed to writing the appendix on instrumentation.

W. R. Perret was Scientific Advisor for the latter portion of the field program.

L. D. Watkins was responsible for electronic integration to give peak displacements and helped considerably to provide prompt data reduction at Sandia.

Frank Adelman of LRL provided scientific liaison between Sandia and theoreticians at LRL and RAND Corporation. All field support was obtained through the LRL engineering staff.

The fast-moving firing program of Project Cowboy was possible only because of the enthusiastic participation of everyone connected with the operation.

CONTENTS

ILLUSTRATIONS

TABLES

Chapter 1

INTRODUCTION

Project Cowboy is an experiment designed to determine to what extent underground explosions can be effectively concealed simply by firing the explosion in a large cavity. Comparative measurements of earth motion were obtained from tamped charges of high explosives and similar yield high explosive charges fired in large cavities in halite. The tamped explosions are referred to as coupled and the explosions in cavities as decoupled shots. The function of the cavity is to decouple the explosion from the surrounding medium and thus conceal the explosion by reducing the amount of energy transmitted to the medium at low frequencies.

Instrumentation was included to measure ground motion, both in the salt near the explosions and on the earth's surface, out to ranges of several miles. Sandia Corporation was responsible for much of the instrumentation within 200 feet of the explosion.

1.1 OBJECTIVE OF CLOSE-IN INSTRUMENTATION

Close-in measurements were required for two main reasons:

1. To indicate the actual pressure-time history on the wall of the cavities, and

2. To show comparative motions of the salt at comparable distances from identical-yield tamped and decoupled explosions.

In the case of the cavity, measurement of the cavity pressure-time history and displacement in the salt medium would provide data to compare with theoretical calculation. Such a comparison would serve to verify that theoretical calculations are accurate. Actually, completely satisfactory

measurement of permanent displacement is difficult to obtain. Peak transient velocities and peak displacements are readily obtainable.

For tamped explosions, the most useful quantity to obtain would be permanent displacement, although, again, transient peak velocities and displacements should also be useful.

1.2 BACKGROUND

The idea that underground explosions can be concealed has been published in a RAND Corporation report.[1] Since the ideas involve a combination of application of elasticity theory to the behavior of cavities in hard rock and experimental observations of motions near a 1.7-kt nuclear explosion (Rainier), it seemed highly desirable to obtain more direct experimental confirmation of the theory. Lawrence Radiation Laboratory was requested to conduct the experiment: Project Cowboy. Sandia Corporation was requested by LRL to provide strong-motion instrumentation within the surrounding rock at certain distances from the explosions.

At the time the experiment was designed (early summer, 1959) we decided to use available commercial instruments because of the planned, short time scale. Since displacement gages were not available, we suggested that primary instrumentation be velocity gages. Use of accelerometers was also planned in the event velocity gages were not adequate; however, the latter were satisfactory. It would have been still better to have invented a good displacement gage; one was built in time for inclusion on two cavity shots.

The experiment was conducted at depths near 800 feet below the surface in the Carey Company salt mine near Winnfield, Louisiana. All instrumentation provided by Sandia was located in the mine. Since both coupled and decoupled shots were fired in the salt medium, factors describing concealment refer to comparable shots in salt.

1.3 THEORY

The ratio of the distant signals in the limit of low frequencies between a tamped and a decoupled explosion is given by Eq. 11 of RAND report R-348.[1]

$$\text{decoupling factor} = \frac{16\pi}{3(\gamma-1)} \quad \frac{c_h}{c} \quad \mu_h \frac{r_o^2 \, d_o}{W} \tag{1.1}$$

where γ = ratio of specific heats applicable to explosion in cavity

c_h = velocity of sound in medium around cavity

c = velocity of sound in medium around tamped shot

μ_h = shear modulus in medium around cavity

r_o = close distance to tamped explosion at which permanent displacement, d_o, is measured in elastic zone

W = explosion energy release

This expression involves the assumption that energy W is distributed uniformly over the cavity volume, giving a step-function pressure, p, on the wall (Eq. 1 of above cited report):[1]

$$p = \frac{(\gamma-1)\, W}{4/3 \; \pi a^3} \tag{1.2}$$

where a is the radius of the cavity.

The Cowboy experiments involved the use of spherical charges of Pelletol (TNT at 1 gm/cc) placed at the center of the cavity which was evacuated to about 1/20 of an atmosphere. The pressure observed at the wall did not turn out to be simply the pressure given by Eq. 1.2. This fact emphasizes the necessity for carrying out the elastic calculation for the Cowboy cavities by using the observed (or accurately calculated) pressure-time history on the cavity wall. That is to say, one cannot, with accuracy, simply

employ Cowboy strong-motion results in Eq. 1.1 unless he ignores the actual pressure measured. Another difficulty also arises in accurate determination of d_o. This problem is discussed in Section 3.2. Nevertheless, observed transient displacements could be calculated to verify that the cavity does behave according to elastic theory.

Equation 1.1 says nothing about the largest W which can be fired in the cavity. One function of the Cowboy experiment was to determine how large W could be, and the close-in measurements served to show whether the motion for large W increased in proportion to W.

Some insight into the experiment can be obtained from an approximate, elementary theory of the behavior of peak velocities and displacements. Assume, in the case of the cavity, that effective pressure on the cavity wall is p_o, and that p_o is low enough in magnitude for pressure at radius r from the center of a cavity of radius to vary as

$$p = p_o \frac{a}{r} \tag{1.3}$$

The 1/r dependence at large r is a valid approximation; see Sharpe.[2] Assume also that

$$p = \rho c u \tag{1.4}$$

where u = peak particle velocity

c = velocity of sound

ρ = density

Equation 1.4 is a close approximation at large r. Then we may write

$$u = \frac{p_o}{\rho c} \frac{a}{r} \qquad r > a \tag{1.5}$$

To the extent that u versus time behaves nearly like a half-pulse of a sine wave, it is permissible to obtain peak displacement from $d = \frac{u}{\omega}$.

If, in addition, it is true that $\omega = \frac{c}{a}$ because of the elastic cavity behavior, then

$$d \propto \frac{p_o}{\rho c^2} \frac{a^2}{r} \qquad r > a \qquad (1.6)$$

(Equations 1.5 and 1.6 will not hold so close to the cavity that the inductive mass motion occurs involving dependence on $1/r$ and $1/r^2$.

For the tamped situation there exists some effective pressure p_{ot} at some effective radius a_t, such that for peak velocities and displacements from the tamped explosions

$$u_t = \frac{p_{ot}}{\rho_t c_t} \frac{a_t}{r} \qquad (1.7)$$

$$d_t \propto \frac{p_{ot}}{\rho_t c_t^2} \frac{a_t^2}{r} \qquad (1.8)$$

To obtain close-in decoupling factors for peak values, we need only look at the observed ratios u_t/u and d_t/d. When $\rho = \rho_t$ and $c = c_t$, as in the Cowboy experiments, we find

$$\frac{u_t}{u} = \frac{p_{ot} \; a_t}{p_o \; a} \qquad r \gg a, \text{ and } a_t \qquad (1.9)$$

$$\frac{d_t}{d} = \frac{p_{ot} \; a_t^2}{p_o \; a^2} \qquad r \gg a, \text{ and } a_t \qquad (1.10)$$

The distant decoupling factor is further increased in proportion to ω_o/ω_{ot}, where $\omega_{ot} = c/a_t$ and $\omega_o = c/a$.[1] Such an increased decoupling would be observed at large distances or close in with low-pass measuring instruments such that $\omega_i \ll \omega_o$. The low-frequency limit of the Fourier transform of displacement related to ω_{ot} is higher than the corresponding limit for ω_o in the ratio ω_o/ω_{ot} to the extent that amplitude and shape of initial driving pressures at the elastic radii are similar.

$$\frac{d_t(\omega_i \ll \omega_o)}{d(\omega \ll \omega_o)} = \frac{p_{ot}\, a_t^3}{p\, a^3} = \text{distant decoupling factor,} \qquad (1.11)$$

where ω_i is related to the instrument.

The ratios

$$\frac{p_{ot}}{p_o} \text{ and } \frac{a_t}{a}$$

are calculable from ratios of observed peak velocities and displacements so that the distant decoupling factor is calculable from Eq. 1.11. However, Eq. 1.10 will apply in case the measuring station has instruments that respond near ω_o and the station is not far enough away for ω_o to be attenuated by solid friction.

In case transient peak pressure on the cavity wall is of large amplitude compared to pressure calculable from Eq. 1.2, and its duration is shorter than a time comparable to $\frac{1}{\omega_o}$, the propagated pressure pulse may not be characterized by ω_o and Eq. 1.6 is not strictly applicable. Nevertheless, Eqs. 1.9 thru 1.11 seem to be useful for understanding strong-motion data obtained on Cowboy. However, the equations do not illustrate why a may be, and usually is, significantly smaller than a_t.

The exact manner in which pressure falls off with distance in salt was not known at the start of Project Cowboy. We did know that in air or soil, in the range of measurement planned for salt, dependence would be r^{-3}, and that for water,[3] dependence has been observed to be $r^{-1.12}$. Presumably, the exponent for salt would be between these, since a dependence near $r^{-2.3}$ had been calculated for nuclear shots in tuff.[4] In calculating velocities to be anticipated, a further difficulty arises since, at close distances, mass motion of material near the explosion introduces an r^{-2} term.

In practice, for the tamped explosion, our method of predicting velocity was to make a guess and hope that we would be correct within a factor of five. After one shot had been fired and measurements obtained at two distances, empirical formulas could be established for prediction for later explosions. For high explosives, the similarity principle can be invoked for different size explosions, so that equal velocities are anticipated at corresponding distances scaled in proportion to $W^{1/3}$. Incidentally, this cannot in general be done for nuclear explosions, since the starting pressure at the edge of the nuclear explosive on the wall of the room depends on the yield of the explosion. In the case of similar high-explosive charges (closely tamped Pelletol was always used for the tamped Cowboy shots), the starting pressure at the edge of the tamped explosion is independent of the yield of the explosion.

Results of the Cowboy tamped explosions soon indicated that we could write the empirical expression for peak velocities: $u \propto r^{-1.65}$ over the range of $r/W^{1/3} = 4$ to 80, where r is in feet and W is yield in pounds. This relation is very likely nearly correct for high explosives in any hard rock.

Consider now the term $r_o^2 d_o$ which occurs in Eq. 1.1. This term represents the permanent mass motion which would occur after an explosion in a perfectly elastic, incompressible medium. That is, the increase in volume of the hole in which the explosion is fired is observable at any distance r_o as a permanent displacement d_o such that the permanent volume change in the charge hole is equal to $4\pi r_o^2 d_o$. The authors of the RAND report[1] were naturally hopeful that we might obtain a good measurement of d_o. The intent was to integrate the velocity-time records. It turned out that this could not be done accurately because the peak displacements were quite large compared to the permanent displacements, even for the tamped explosions. This problem is discussed in detail later. It is mentioned here to point out that the assumption that a tamped explosion injects a step function of pressure at some elastic radius is only valid for frequency components much lower than the dominant information frequency as observed close to the explosion. This is a basic assumption of the decoupling theory.

The above discussion should serve to show that primary close-in measurements should be (a) pressure versus time at the cavity wall, and (b) velocities and displacements in the medium near tamped and decoupled explosions. Of course, the distant seismic signals provide direct measurement of decoupling factors, modified by the response and location of the seismometers.

Chapter 2

DESCRIPTION OF EXPERIMENT

2.1 INSTRUMENT LAYOUT

Plan views of instrument locations with respect to the 6-foot and 15-foot radius cavities are shown in Figs. 2.1 and 2.2. Gages were similarly placed for tamped explosions. Figure 2.3 shows an overall plan of the Cowboy experimental area as located in the Carey Salt Company mine.

In the case of the 15-foot radius cavity, four pressure gages were used to indicate pressure as a function of time. Two of these gages were located in a plate near the entrance to the cavity. The other two were placed 45 degrees and 90 degrees away on the horizontal great circle. After the 500-pound shot was fired, strain gages were placed over a 3-foot span of a great circle to read circumferential strain of the cavity wall. A pressure gage with a long fill time was employed to read pressure in the cavity at long times compared to the duration of the transient pressure pulse. An armored thermocouple was placed to project about three-eights of an inch into the cavity to give an indication of the cavity wall temperature. Of course, it could not follow the transient high temperature ($\sim$ 3000 degrees K) of the gaseous explosion products, but it did indicate roughly the wall temperature and how rapidly cooling took place.

Details about instruments and instrument placement are described in Appendix A. The gages were placed so as to read radial motion except in the case of the cavity wall strain.

2.2 DATA REDUCTION PROCEDURE

The primary method of recording data was frequency-modulation recording on magnetic tape. A secondary method was directly recording on photographic

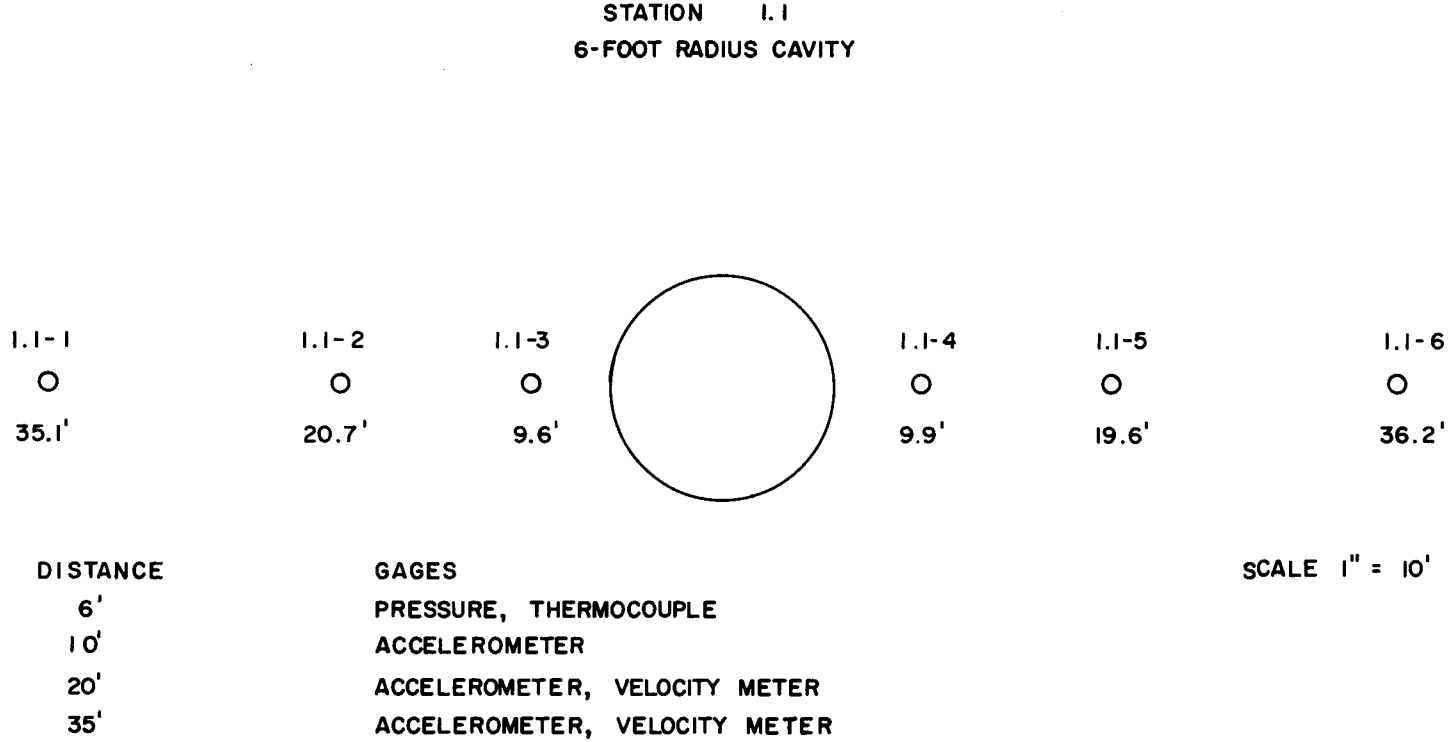

Fig. 2.1 Schematic gage layout near 6-foot cavity

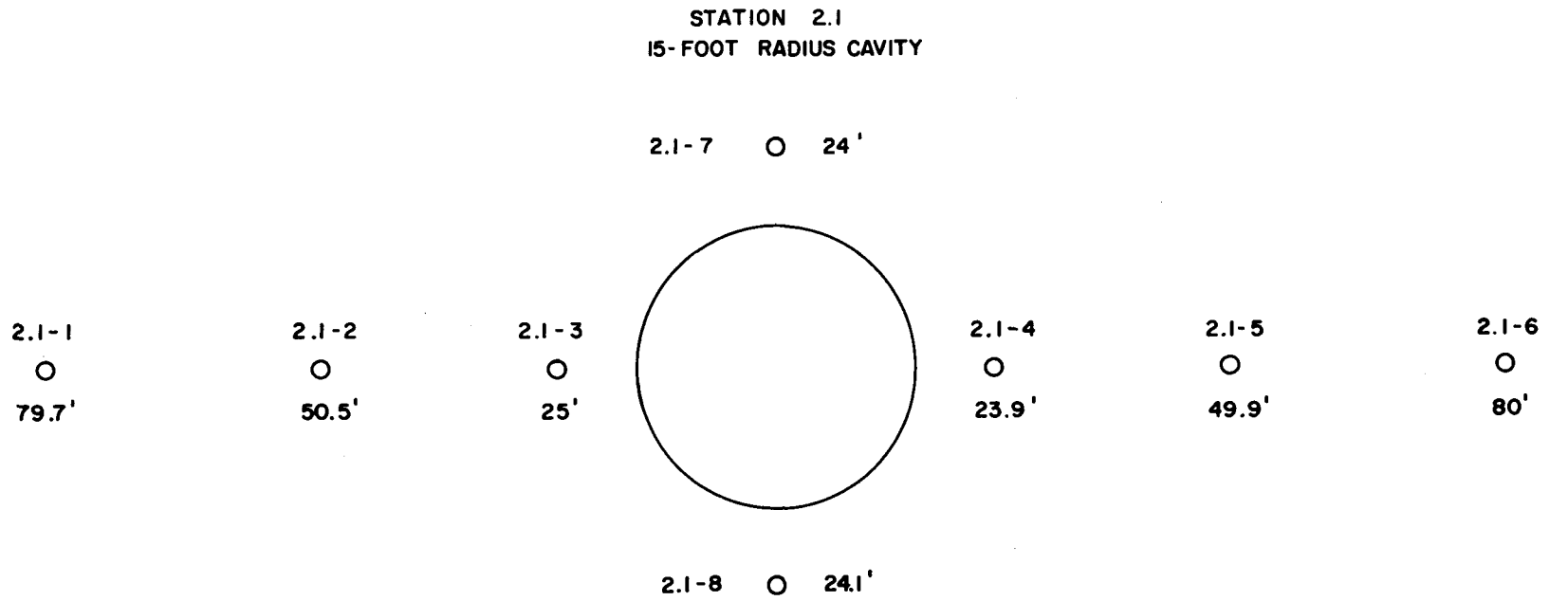

Fig. 2.2 Schematic gage layout near 15-foot cavity

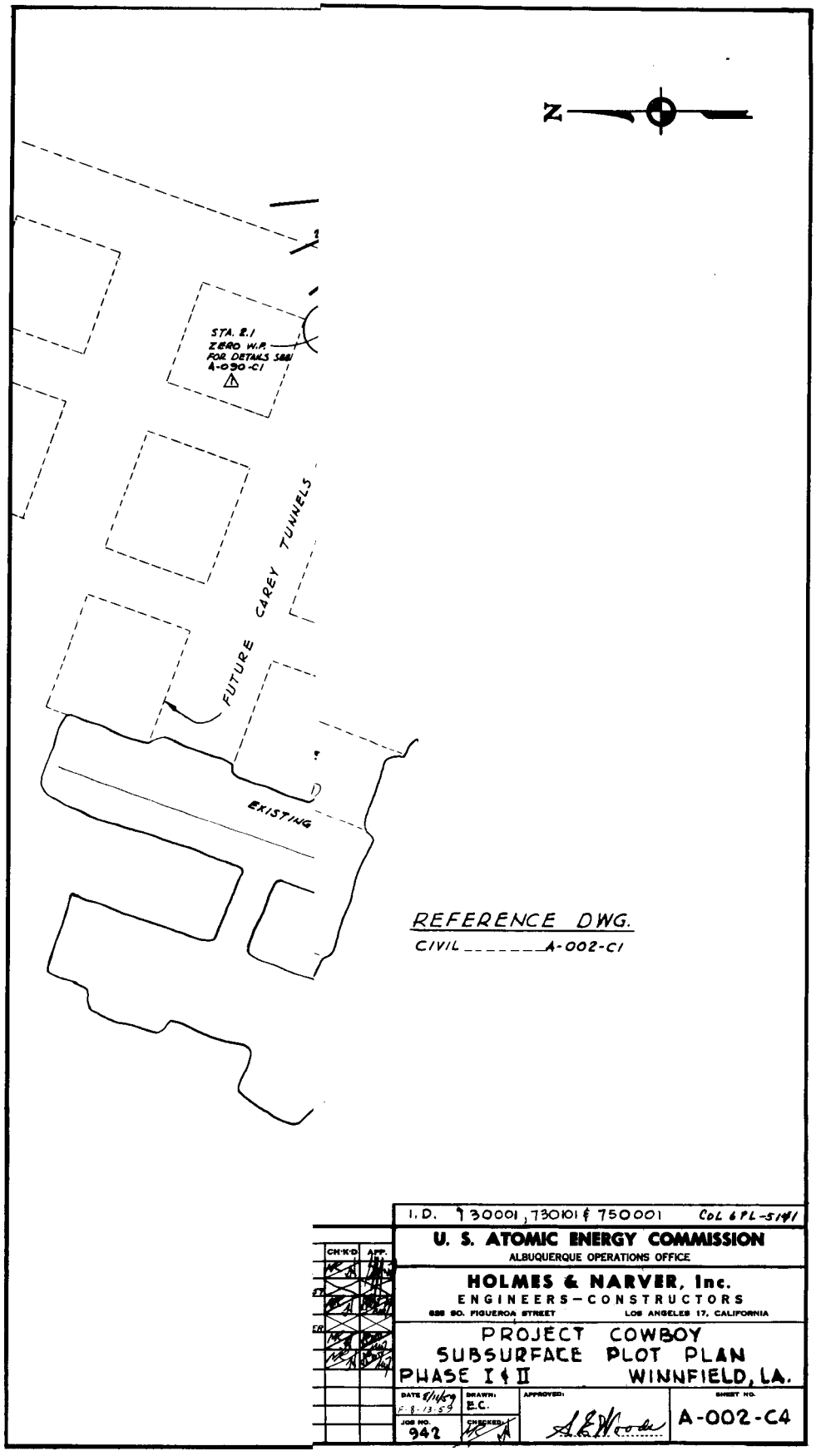

REFERENCE DWG.
CIVIL _____ A-002-C1

I.D. 730001, 730101 & 750001 COL 6 PL-5141

U. S. ATOMIC ENERGY COMMISSION
ALBUQUERQUE OPERATIONS OFFICE

HOLMES & NARVER, Inc.
ENGINEERS—CONSTRUCTORS
626 SO. FIGUEROA STREET LOS ANGELES 17, CALIFORNIA

PROJECT COWBOY
SUBSURFACE PLOT PLAN
PHASE I & II WINNFIELD, LA.

CH'K'D	APP.

DATE 8/14/59 (F 8-13-59)
DRAWN: E.C.
JOB NO. 942
CHECKED:
APPROVED: A.E. Woods
SHEET NO. A-002-C4

film (velocities only) from "string" galvanometers. The purpose of this was to try to reduce the noise level which so greatly affects integration to long times. On two occasions LRL provided sweep oscillographs and recorded pressure versus time on the cavity wall to provide frequency response beyond gage capability.

Nearly all data were played back in the field by means of a Visicorder to provide immediate documentation. Integration of velocities to give peak displacement was done in the field by means of an integrating network. Copies of these playbacks were given to the Technical Director, together with our field analysis of peak values. All previously published peak values of velocities or of integrated displacements are those which we read in the field.

Immediately after field playback, all recordings were sent to the Data Reduction Division at Sandia Laboratory for final playback, integration, and reproduction. Copies of these final playbacks have already been distributed to LRL, RAND, AWRE, and Sandia. All final playbacks have calibration signals preceding the recording, as well as readings of peak values as read according to our initial judgment. This problem of judgment in reading occurs mainly in connection with peak pressures in the cavity and with peak velocities for small explosions in the cavity.

Velocity recordings were integrated electronically to give records of displacement versus time. Such integration is naturally limited in low-frequency response and does not give accurate permanent displacements, inasmuch as the circuitry requires that the signal came back to zero. For this reason and in an effort to improve signal-to-noise ratio, signals from velocity

gages were also recorded by means of galvanometers. Velocities so recorded were read by data reduction analysts and were integrated by means of a computer. Listings of velocity and displacement versus time have also been supplied to LRL, RAND, AWRE, and Sandia. Actually, permanent displacements obtained in this way are not as accurate as desired. All velocity-versus-time recordings have now been played back successively through various low-pass filters to demonstrate that low-frequency displacements are lost in the "noise." Results are discussed in Chapter 3.

Dynamic range better than 1000 to 1 is required to obtain reliable permanent displacement information from integration of velocity-time recordings. Such accuracy is very difficult to achieve in experiments of this sort and was not designed into the experiment at the outset. In experiments such as Cowboy, theoretical analysis should, if at all possible, be designed to deal with peak values. By the time uncertainties in signal amplitudes to be expected are taken into account, it is, in practice, difficult to obtain signals with 10-percent accuracy which are, at the same time, thirty to fifty times the noise level. Sandia instrumentation on Cowboy was designed to give a dynamic range of about 100 to 1 under the optimum condition of a full-scale signal.

Chapter 3

RESULTS

About 300 recordings, as a function of time, were made by Sandia of the 17 high-explosive shots fired between December 17, 1959, and March 4, 1960. These recordings have been severely edited and the most useful ones have already been furnished to theoretical physicists at LRL and RAND Corporation for further analysis.

All the records will not be reproduced in this text, but many examples will be illustrated. Lists and plots of data in the following pages follow the scheme that all data from tamped explosions can be treated as a single unit, but that each explosion in a cavity is best considered individually. Total data from tamped explosions are used in providing comparison with decoupled explosions. Except for one cavity shot (No. 5) and two tamped shots (Nos. 16 and 17), tamped and decoupled shots took place in pairs so that comparative seismic data could be obtained. The schedule, coding, and charge weights of the shots are shown in Table 3.1.

3.1 PEAK VELOCITIES AND PEAK DISPLACEMENTS

Values of observed peak velocities and peak displacements for all explosions are listed in Tables 3.2, 3.3, and 3.4. Except for the gages listed as -DR, all peak displacements were obtained by integrating velocity-time recordings. The -DR gages are experimental displacement gages which were installed late in the program.

Peak velocities and displacements observed for the three 200-pound tamped explosions are plotted in Fig. 3.1 to illustrate the degree to which

TABLE 3.1--SUMMARY OF SHOT DATA - PROJECT COWBOY

Shot no.	Date	Time (CST)	Yield (lbs)	Station	Type
1	17 Dec	0015	20	1.2	Coupled, 45-ft hole
2	17 Dec	0045	20	1.1	Decoupled, 12-ft dia. sphere
3	19 Dec	0000	100	1.1	Decoupled, 12-ft dia. sphere
4	19 Dec	0015	100	1.3	Coupled, 45-ft hole
5	23 Jan	0000:00.113	198.35	2.1	Decoupled, 30-ft dia. sphere
6	30 Jan	0001:00.112	200.0	2.1	Decoupled, 30-ft dia. sphere
7	30 Jan	0101:00.112	199.65	2.2	Coupled, 110-ft hole
8	6 Feb	0001:00.115	477.4	2.1	Decoupled, 30-ft dia. sphere
9	6 Feb	0101:00.113	499.7	2.3	Coupled, 110-ft hole
10	13 Feb	1901:00.113	954.0	2.1	Decoupled, 30-ft dia. sphere
11	13 Feb	2001:00.114	1003.0	2.4	Coupled, 110-ft hole
12	20 Feb	0001:00:112	929.0	1.1	Decoupled, 12-ft dia. sphere
13	20 Feb	0100:59.614	987.6	2.5	Coupled, 110-ft hole
14	27 Feb	0001:00.127	1902.4	1.1	Decoupled, 12-ft dia.sphere
15	28 Feb	0401:00.131	936.2	2.6	Coupled, 110-ft hole
16	3 Mar	2301:00.128	199.5	1.4	Coupled, 45-ft hole
17	4 Mar	0001:00.130	199.8	1.3-1	Coupled, 45-ft hole

Note: (1) All times for shots 5 through 17 are derived from comparisons with WWV. Accuracies are $\pm$ 0.001 sec, except for shot 15, which is $\pm$ 0.003 sec.

(2) All yields include "Nitramon" booster and detonator weights of either 2 or 3 pounds.

TABLE 3.2--PEAK VELOCITIES AND DISPLACEMENTS - TAMPED EXPLOSIONS

Gage	Distance (feet)	Shot No.	W (lbs)	Peak Vel. (in/sec)	$W^{1/3}$	Peak Displ. (mils)		$Mils/W^{1/3}$	$D/W^{1/3}$
1.2-3-V	19.4	1	20	12	2.71	--			7.15
1.2-4-V	36			9.4			low		13.3
1.3-7-V	19.3	4	100	90	4.64	--			4.16
1.3-8-V	35.9			28.4		--			7.73
2.2-3-V	49	7	200	40	5.84	24		4.11	8.4
2.2-2-V	50.3			42		26		4.46	8.6
2.2-1-V	79.4			15.5		10.4		1.79	13.6
2.2-4-V	80.6			10		8		1.37	13.8
2.1-17-VB	452.5			1.0		1.0		0.172	77.5
1.2-4-V	157	16	200	3.9	5.84	3.0		0.515	26.9
1.2-3-V	173			3.0		2.3	low	0.395	29.7
1.3-7-V	223			3.4		2.5		0.429	38.2
1.3-8-V	207			3.7		2.5		0.429	35.5
2.1-17-VB	431			1.1		0.8		0.137	73.8
2.1-17-VC	431			1.0		0.8		0.137	73.8
1.3-7-V	99	17	200	11.2	5.84	8.2		1.4	17
1.3-8-V	116			9.1		8.1		1.39	19.9
1.2-3-V	150			4.4		3.4		0.583	25.7
1.2-4-V	167			4.1		3.2		0.55	28.6
2.1-17-VC	274			1.8		1.5		0.257	47
2.3-2-V	50.5	9	500	48	7.92	48		6.07	6.38
2.3-1-V	79.6			20		22.5		2.85	10
2.3-4-V	79.7			23		20		2.53	10
2.1-17-VB	368.8			2.0		2.9		0.37	46.6
2.4-1-V	77.5	11	1000	46	10	42		4.2	7.75
2.4-15-V	208.2			6.5		9.3		0.93	20.8
2.4-15-DR				--		11.6		1.16	20.8
2.1-17-VB	477.7			2.1		3.2		0.32	47.8
2.5-4-V	80.9	13	1000	40		39		3.9	8.1
2.4-15-V	351.7			4.3		5.6		0.56	35.2
2.4-15-DR				--		6.1		0.61	35.2
2.1-17-VB	585.5			1.3		1.7		0.17	58.6

TABLE 3.3--PEAK VELOCITIES AND DISPLACEMENTS - 15-FOOT CAVITY

Gage	Distance (feet)	Shot No.	W (lbs)	Peak Vel. (in/sec)	Peak Displ. (mils)
2.1-2-V	50.5	5	200	1.4	0.53
2.1-1-V	79.7			0.45	0.25
2.1-4-V	23.9	6	200	2.2	1.44
2.1-2-V	50.5			1.0	0.5
2.1-1-V	79.7			0.4	0.25
2.1-6-V	80			0.4	0.26
2.1-11-V	200.1			0.17	0.09
2.1-4-V	23.9	8	500	7.8	2.5
2.1-2-V	50.5			3.8	1.2
2.1-5-V	49.9			3.4	1.2
2.1-5-DR	49.9			--	1.2
2.1-1-V	79.7			2.0	0.55
2.1-6-V	80			1.6	0.5
2.1-11-V	200.1			0.6	0.2
2.1-17-VA	366.6			0.28	0.1
2.1-4-V	23.9	10	1000	13	5
2.1-5-V	49.9			5.1	1.8
2.5-5-DR				--	2.2
2.1-2-V	50.5			6	2.1
2.1-1-V	79.7			2.6	0.9
2.1-6-V	80			2.4	0.6
2.1-11-V	200.1			0.83	0.28
2.1-17-VA	366.6			0.4	0.14

TABLE 3.4--PEAK VELOCITIES AND DISPLACEMENTS - 6-FOOT CAVITY

Gage	Distance (feet)	Shot No.	W (lbs)	Peak Vel. (in/sec)	Peak Displ. (mils)
1.1-2-V	20.7	3	20	0.7	--
1.1-1-V	35.1			0.5	--
1.1-6-V	36.2			0.45	--
1.1-5-V	19.6	4	100	3.4	--
1.1-2-V	20.7			2.1	--
1.1-1-V	35.1			1.3	--
1.1-6-V	36.2			1.9	--
1.1-5-V	19.6	12	929	32	21.3
1.1-2-V	20.7			24.5	16
1.1-1-V	35.1			12.5	6.7
1.1-6-V	36.2			10.5	7.8
1.1-9-V2	100.7			4	2.4
2.1-17-VB	461.2			0.3	0.3
1.1-5-V	19.6	14	1903.4	71	52
1.1-2-V	20.7			54	43
1.1-1-V	35.1			26.5	18.5
1.1-6-V	36.2			27	19
1.1-9-V2	100.7			6.7	5.5
2.1-17-VB	461.2			0.6	0.6

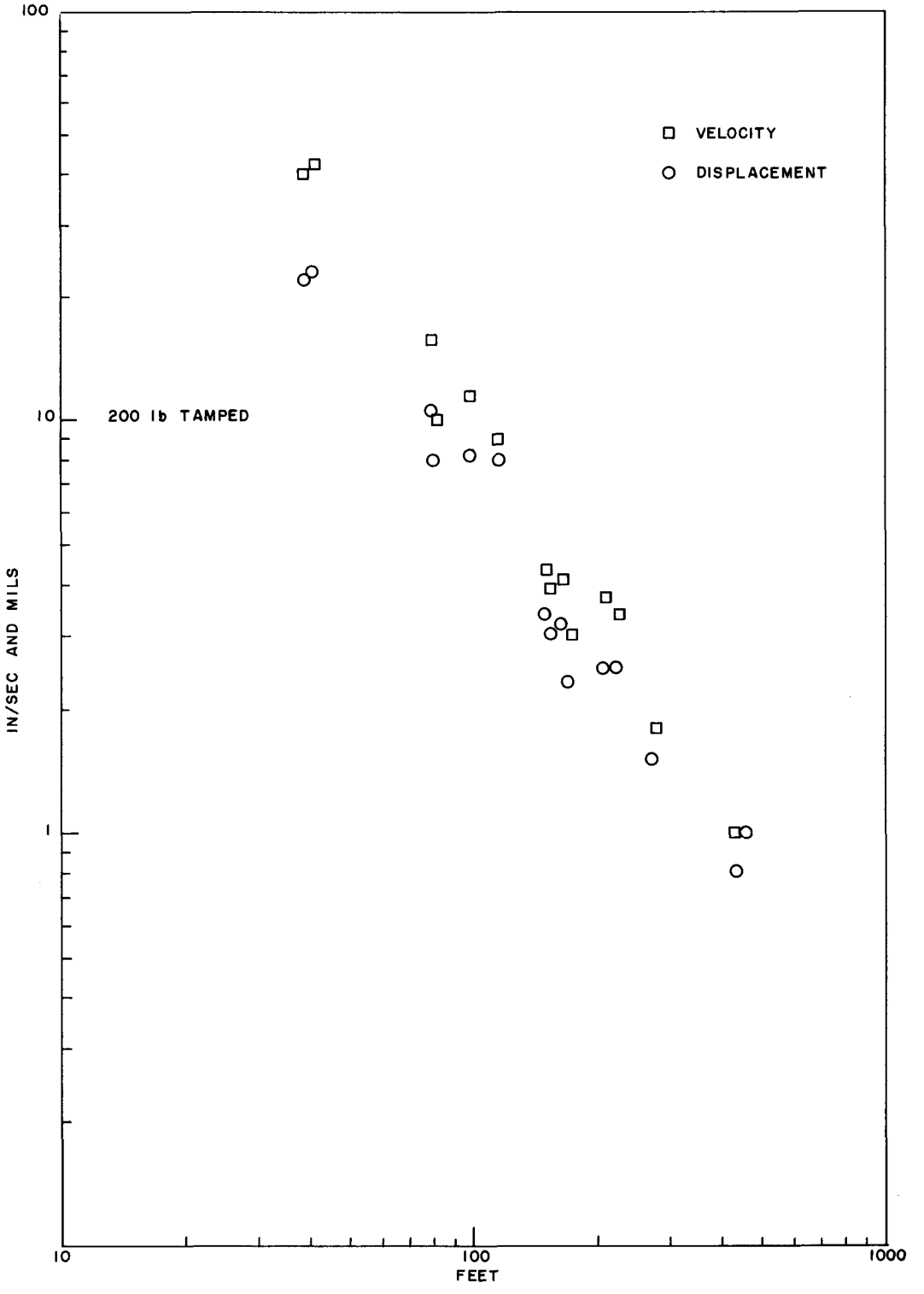

Fig. 3.1 Peak velocities and displacements versus distance for 200-pound tamped explosions

the data are consistent. An example of a velocity-time recording and the corresponding integration is shown in Fig. 3.2.

All peak-velocity data for tamped explosions (20 pounds through 1000 pounds) have been plotted in Fig. 3.3 as a function of distance divided by the cube root of the charge weight. This plot shows that, over the range of scaled distances from 4 to 80, peak velocities fall off with distance (r) as $r^{-1.65}$.

Similarly, Fig. 3.4 is a plot of observed peak displacements for all tamped explosions. However, peak displacement divided by $W^{1/3}$ must be used in the scaled plot. $D/W^{1/3}$ is found to depend on distance as $r^{-1.5}$.

In making comparisons with peak velocities and displacements observed for shots fired in the 6- and 15-foot radius cavities, the best fit to the total sum of tamped data is used. Thus, experimental data for each tamped shot are not shown in the following figures, which illustrate observed peak velocities and displacements for cavity shots in comparison with data from tamped explosions:

Figure 3.5 Peak Velocities, 20 pounds, 6-foot cavity

Figure 3.6 Peak Velocities, 100 pounds, 6-foot cavity

Figure 3.7 Peak Velocities, 929 pounds, 6-foot cavity

Figure 3.8 Peak Displacements, 929 pounds, 6-foot cavity

Figure 3.9 Peak Velocities, 1900 pounds, 6-foot cavity

Figure 3.10 Peak Displacements, 1900 pounds, 6-foot cavity

Figure 3.11 Peak Velocities, 200 pounds, 15-foot cavity

Figure 3.12 Peak Displacements, 200 pounds, 15-foot cavity

Figure 3.13 Peak Velocities, 500 pounds, 15-foot cavity

Figure 3.14 Peak Displacements, 500 pounds, 15-foot cavity

Figure 3.15 Peak Velocities, 1000 pounds, 15-foot cavity

Figure 3.16 Peak Displacements, 1000 pounds, 15-foot cavity

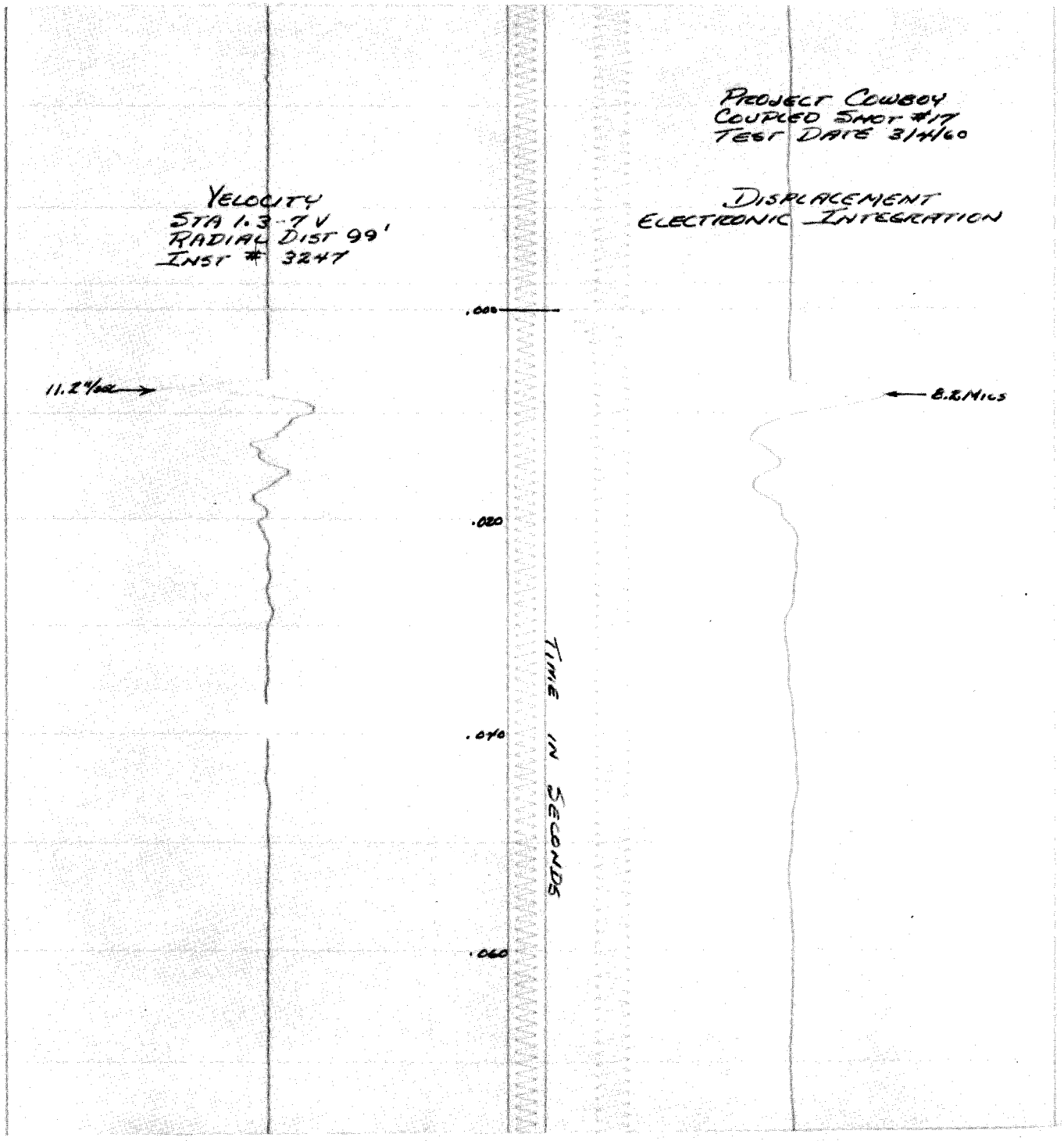

Fig. 3.2 Velocity-time recording and corresponding integration

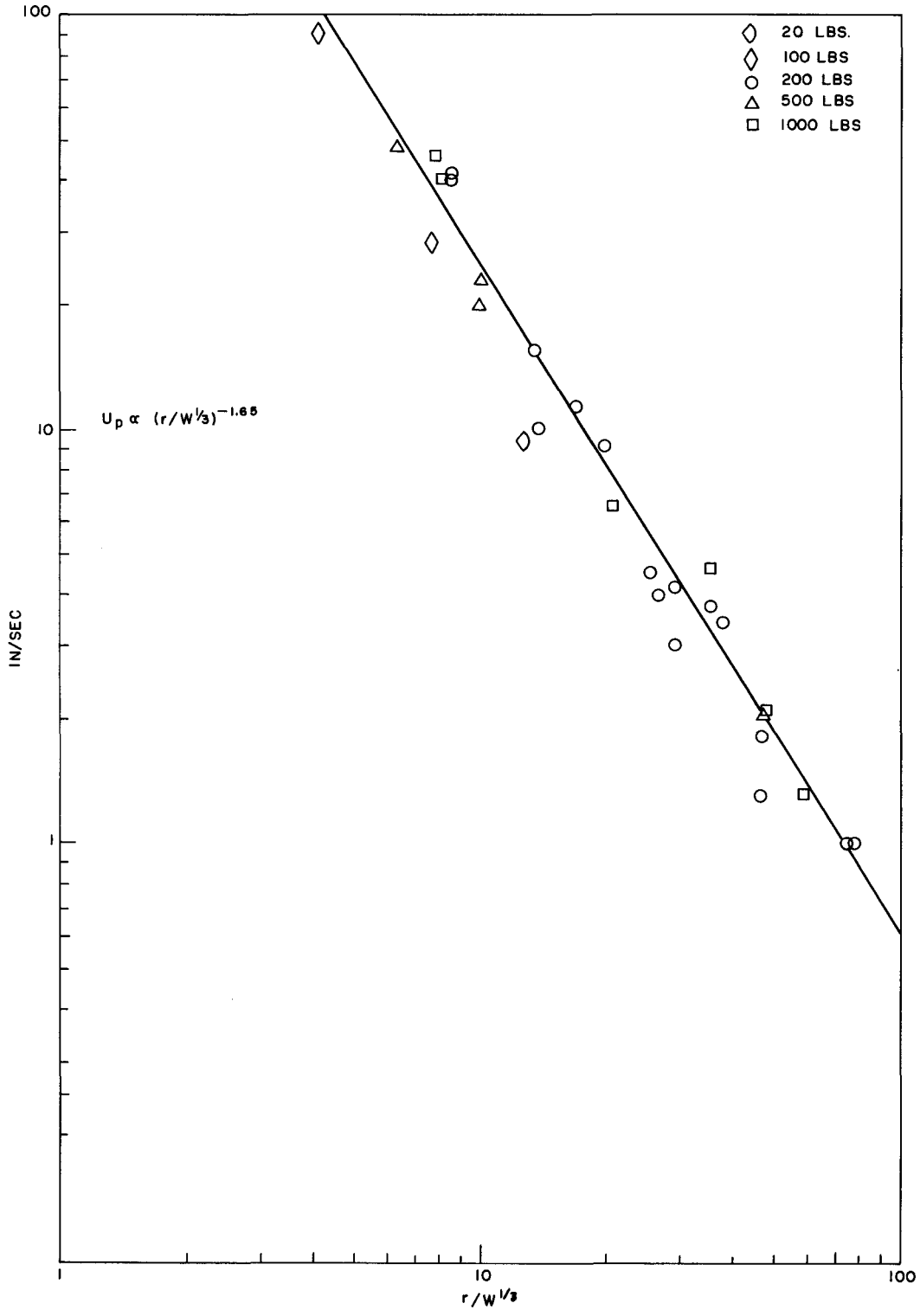

Fig. 3.3 Peak velocity versus Distance/$W^{1/3}$ for all tamped explosions

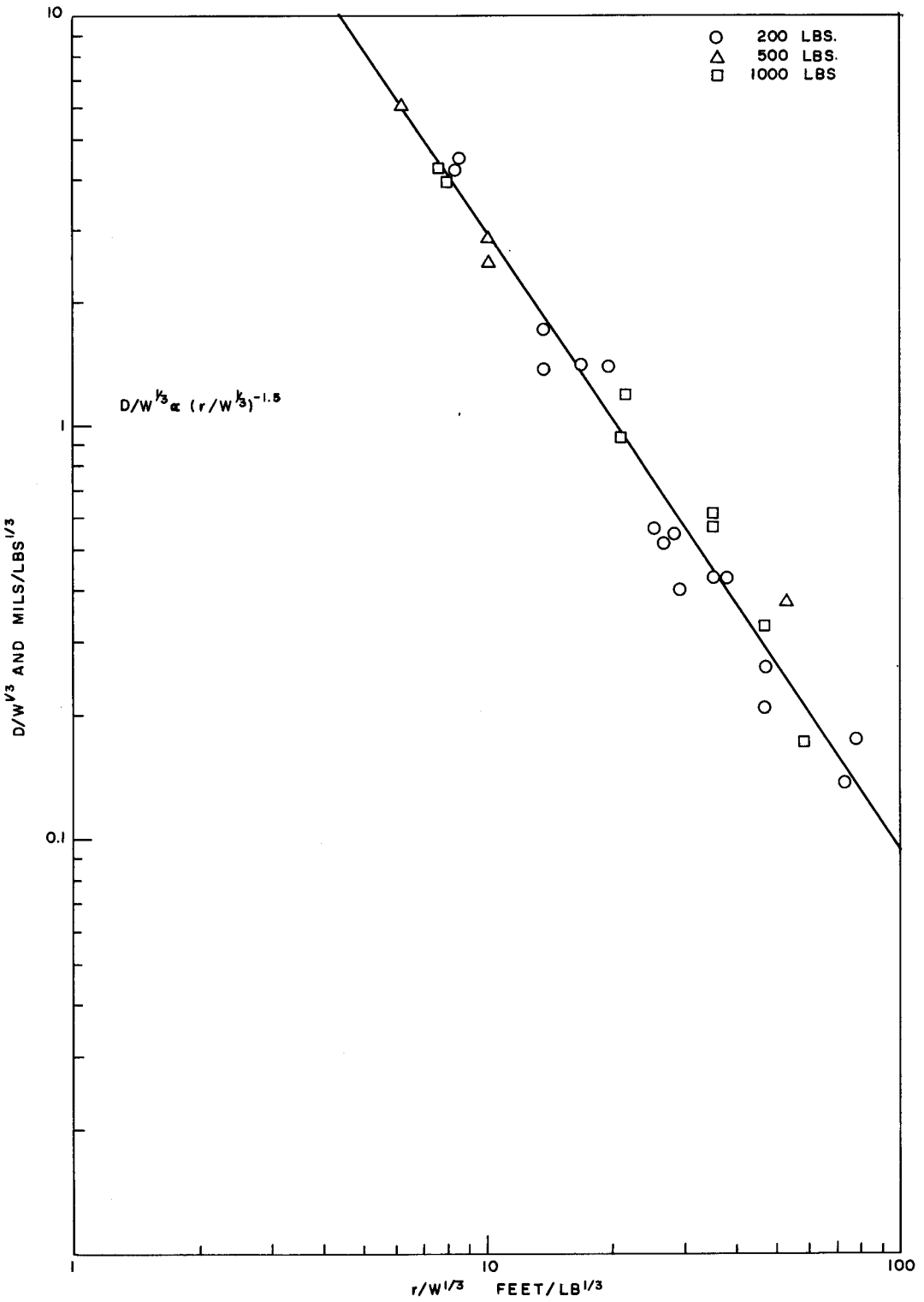

Fig. 3.4 Scaled peak displacements versus scaled distance for all tamped explosions

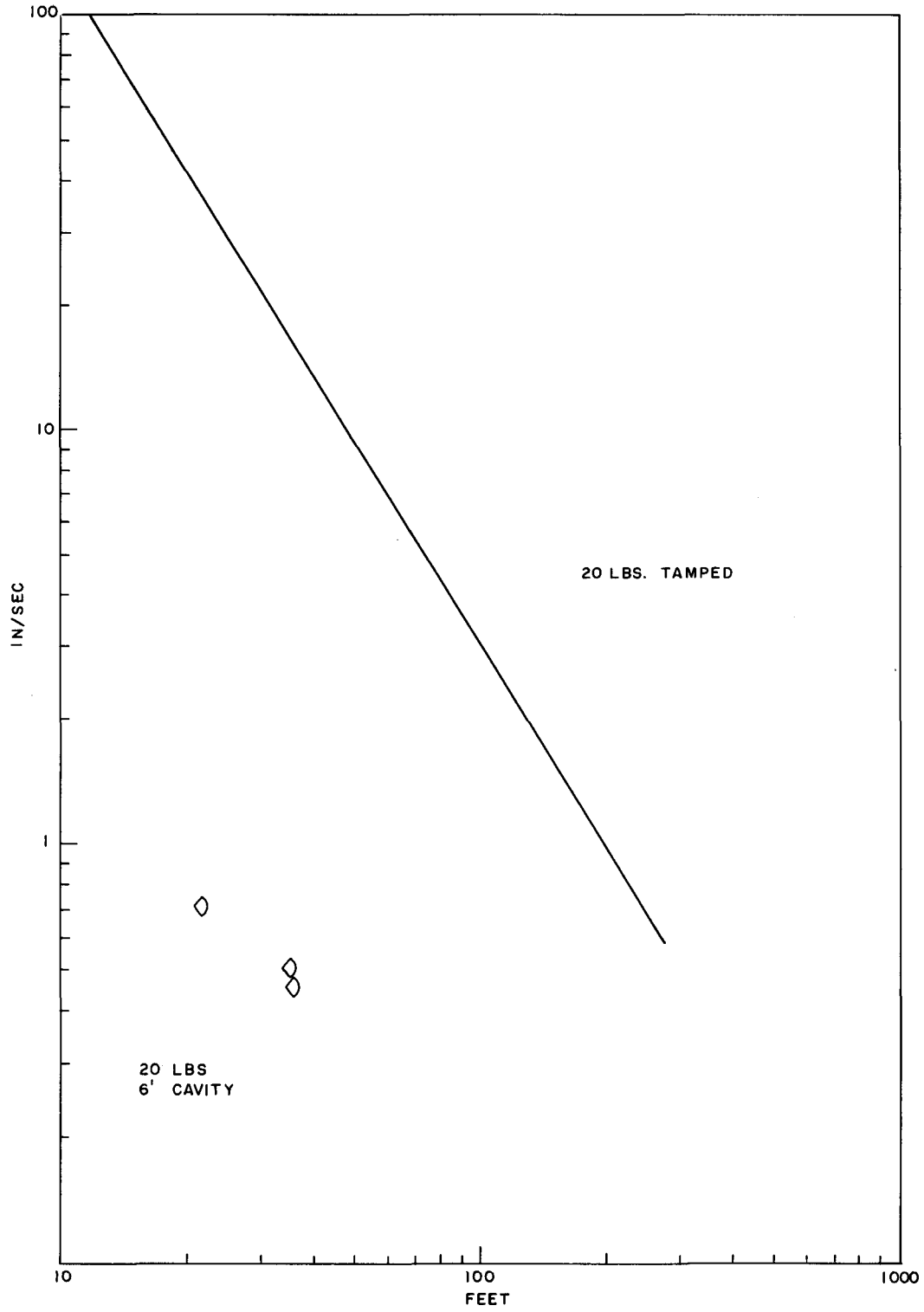

Fig. 3.5 Peak particle velocities versus distance, 20 lbs, 6-ft cavity

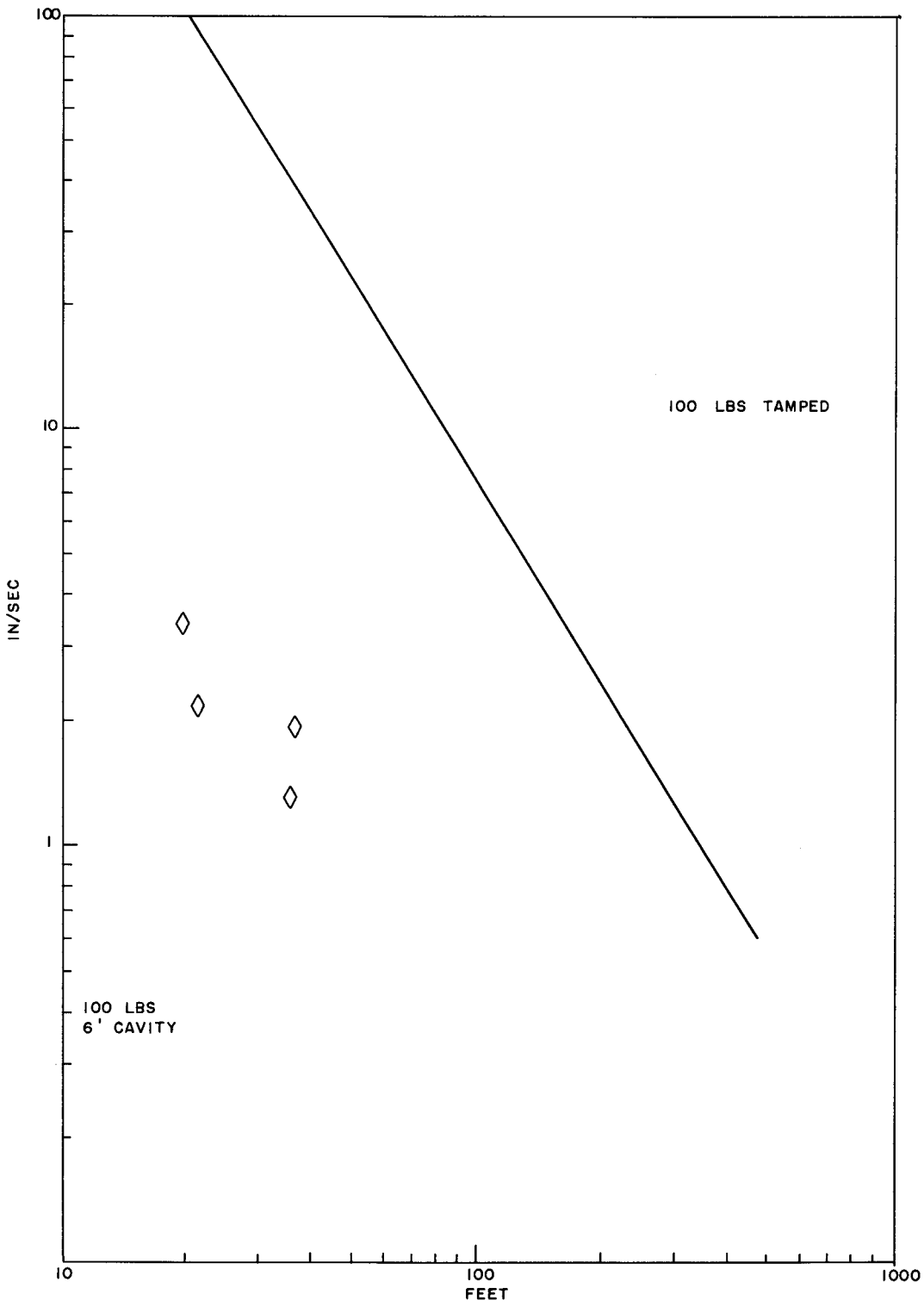

Fig. 3.6 Peak particle velocities versus distance, 100 lbs, 6-ft cavity

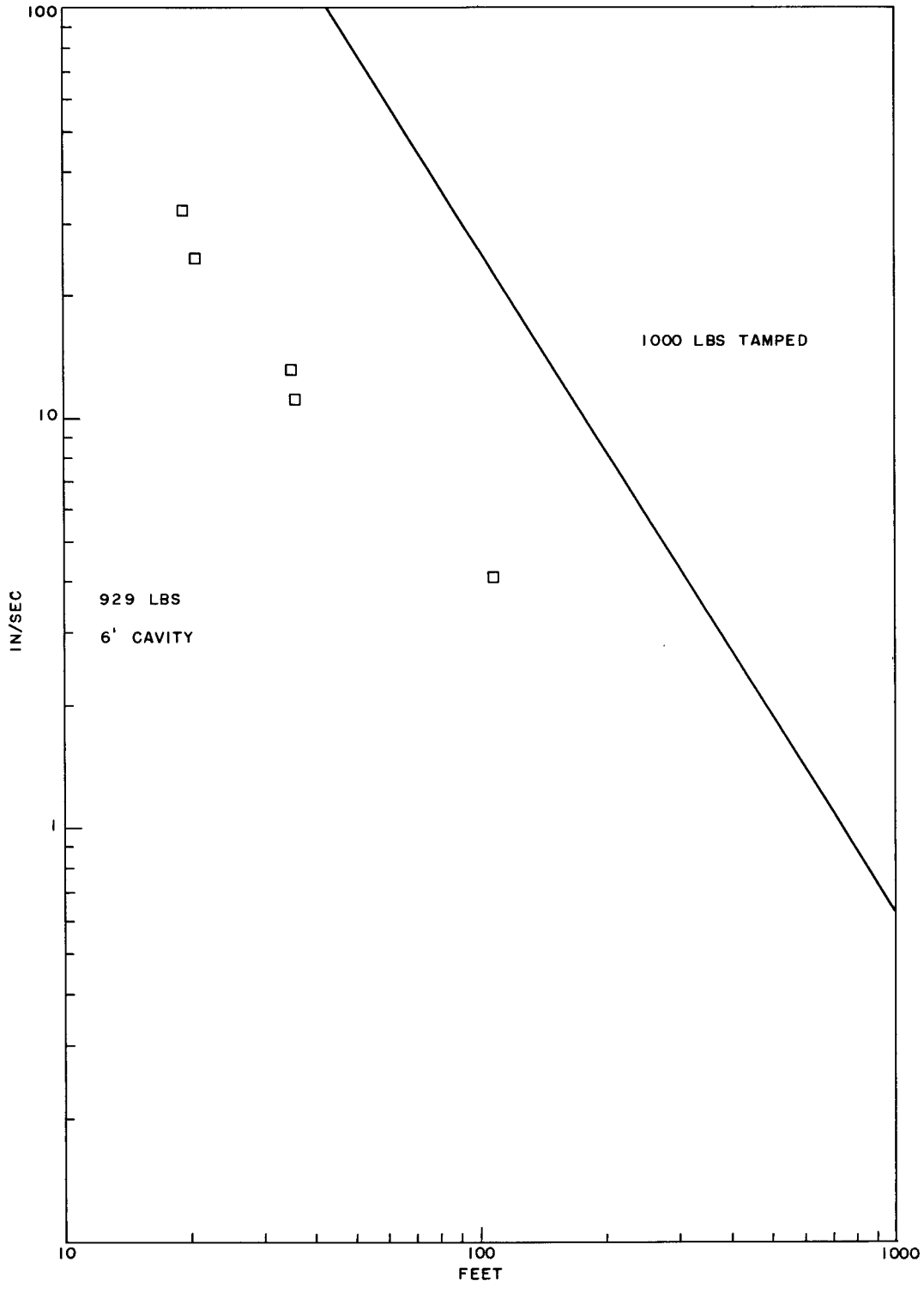

Fig. 3.7 Peak particle velocities versus distance, 929 lbs, 6-ft cavity

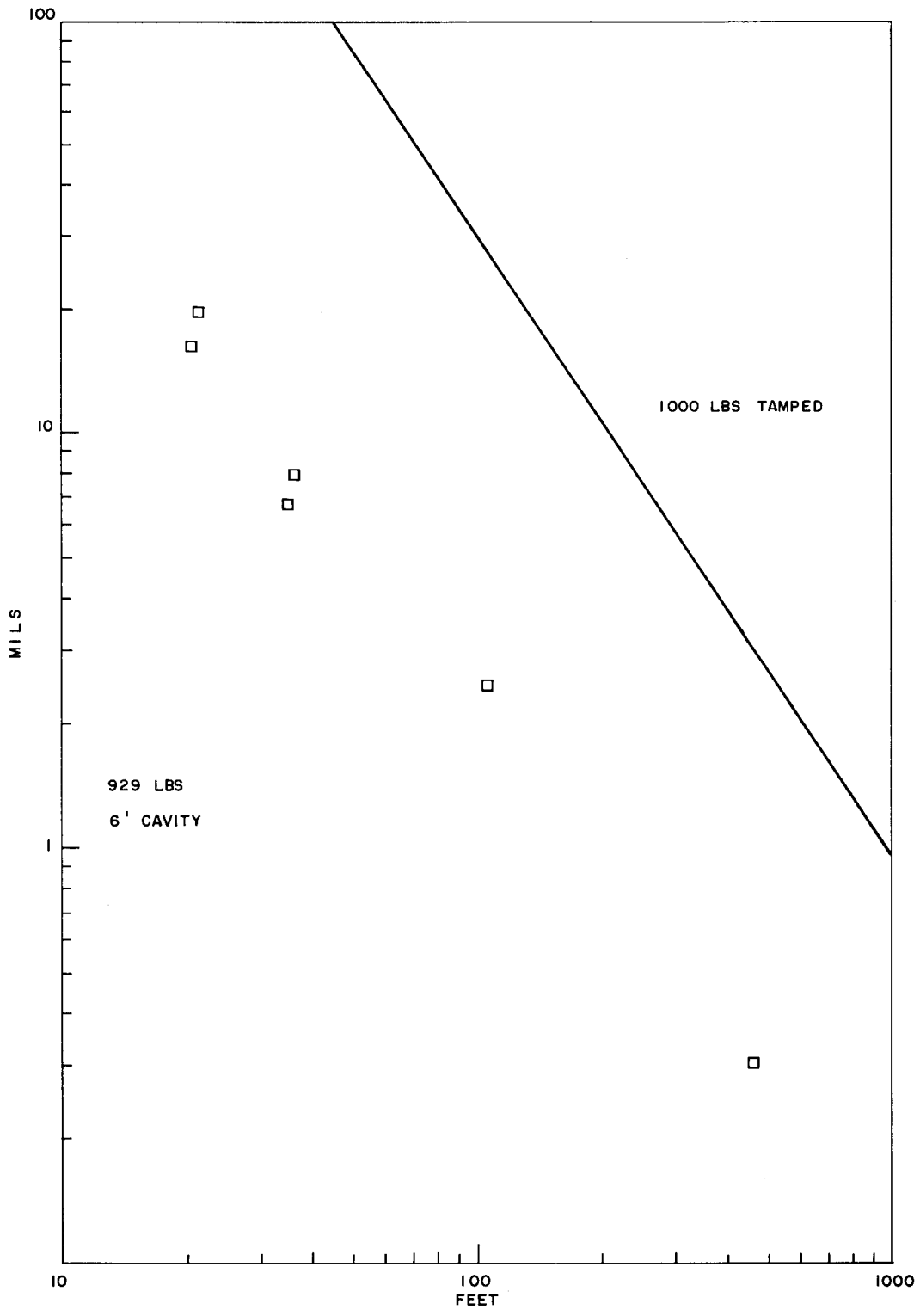

Fig. 3.8 Peak displacement versus distance, 929 lbs, 6-ft cavity

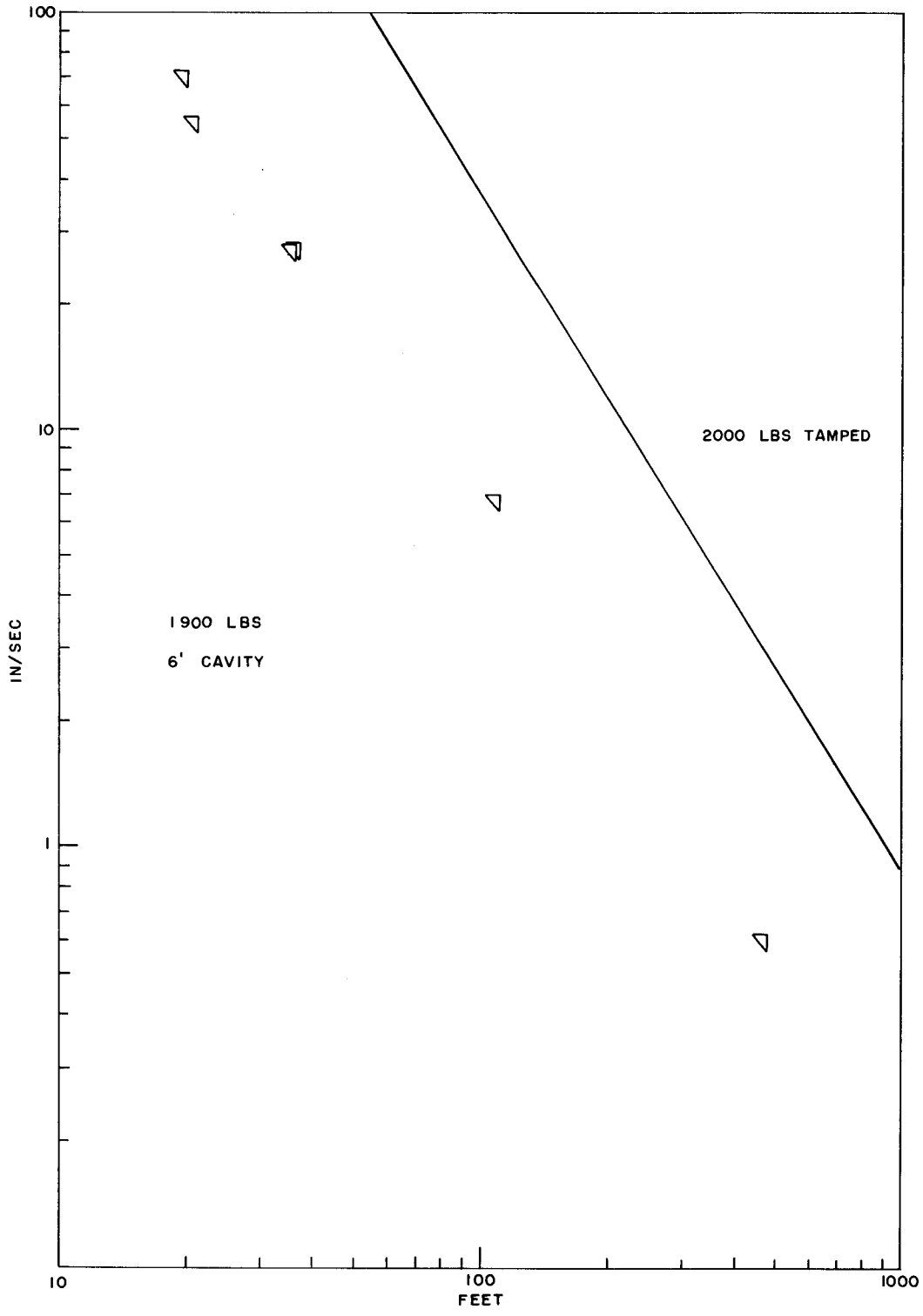

Fig. 3.9 Peak particle velocities versus distance, 1900 lbs, 6-ft cavity

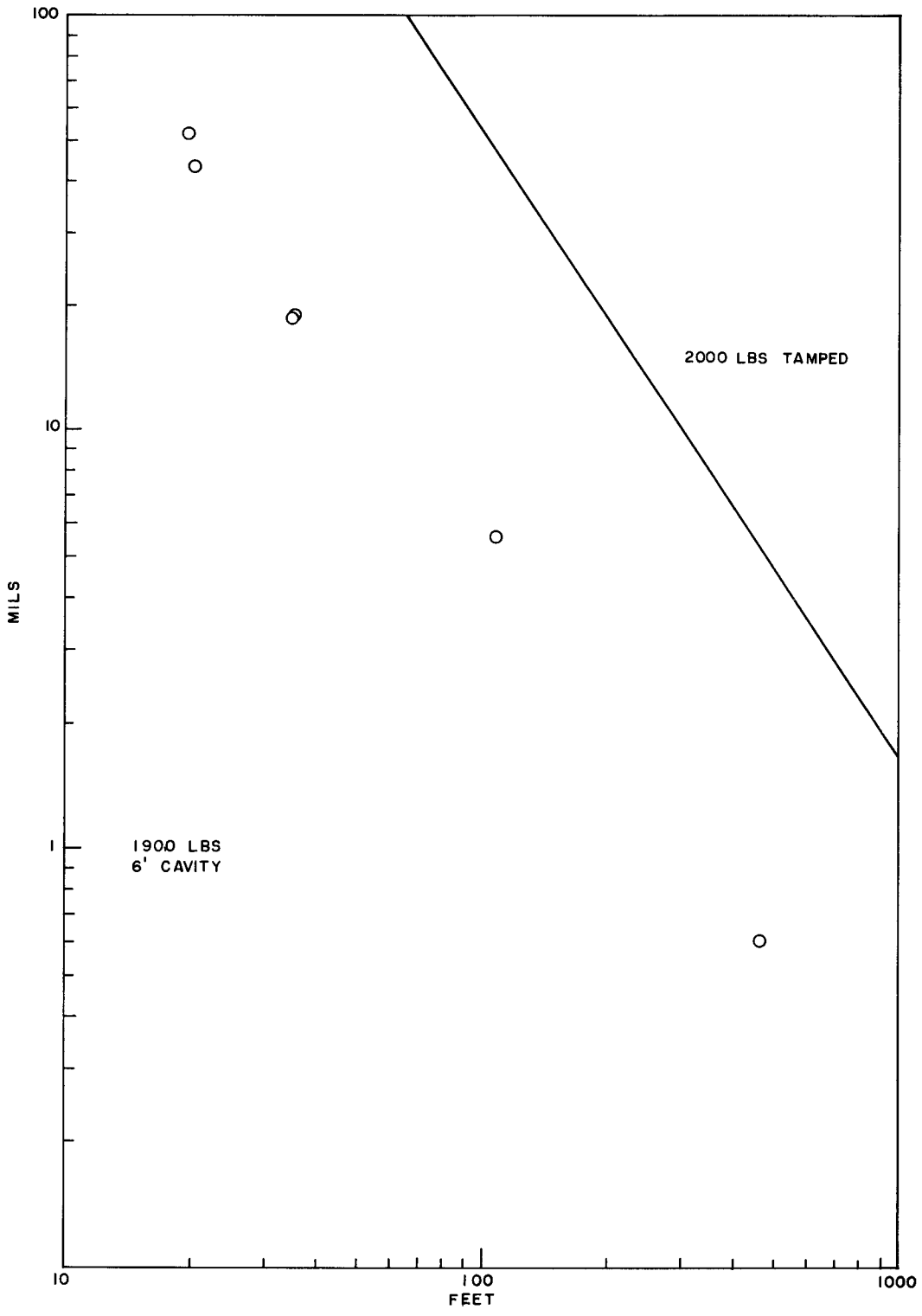

Fig. 3.10 Peak displacement versus distance, 1900 lbs, 6-ft cavity

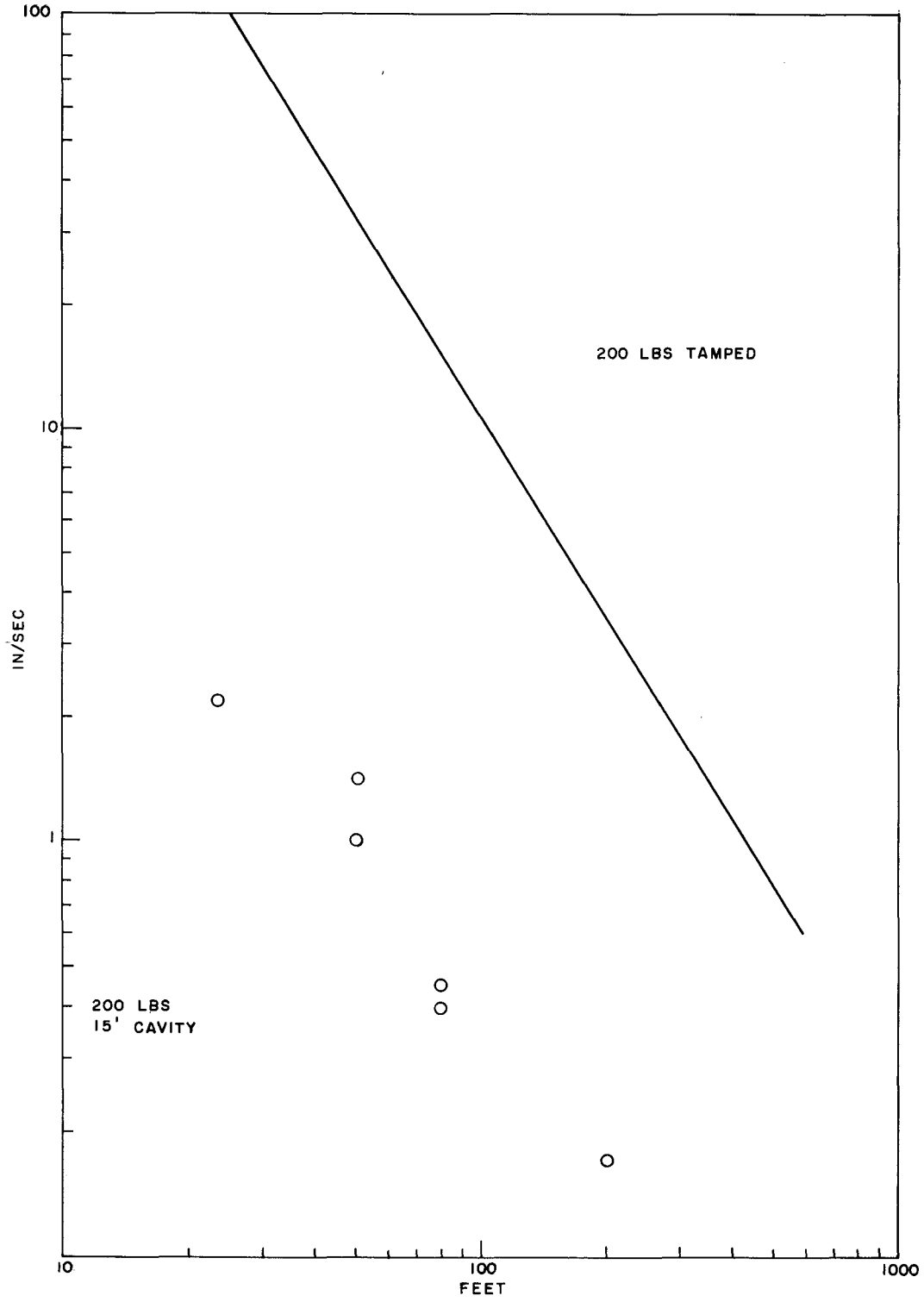

Fig. 3.11 Peak particle velocities versus distance, 200 lbs, 15-ft cavity

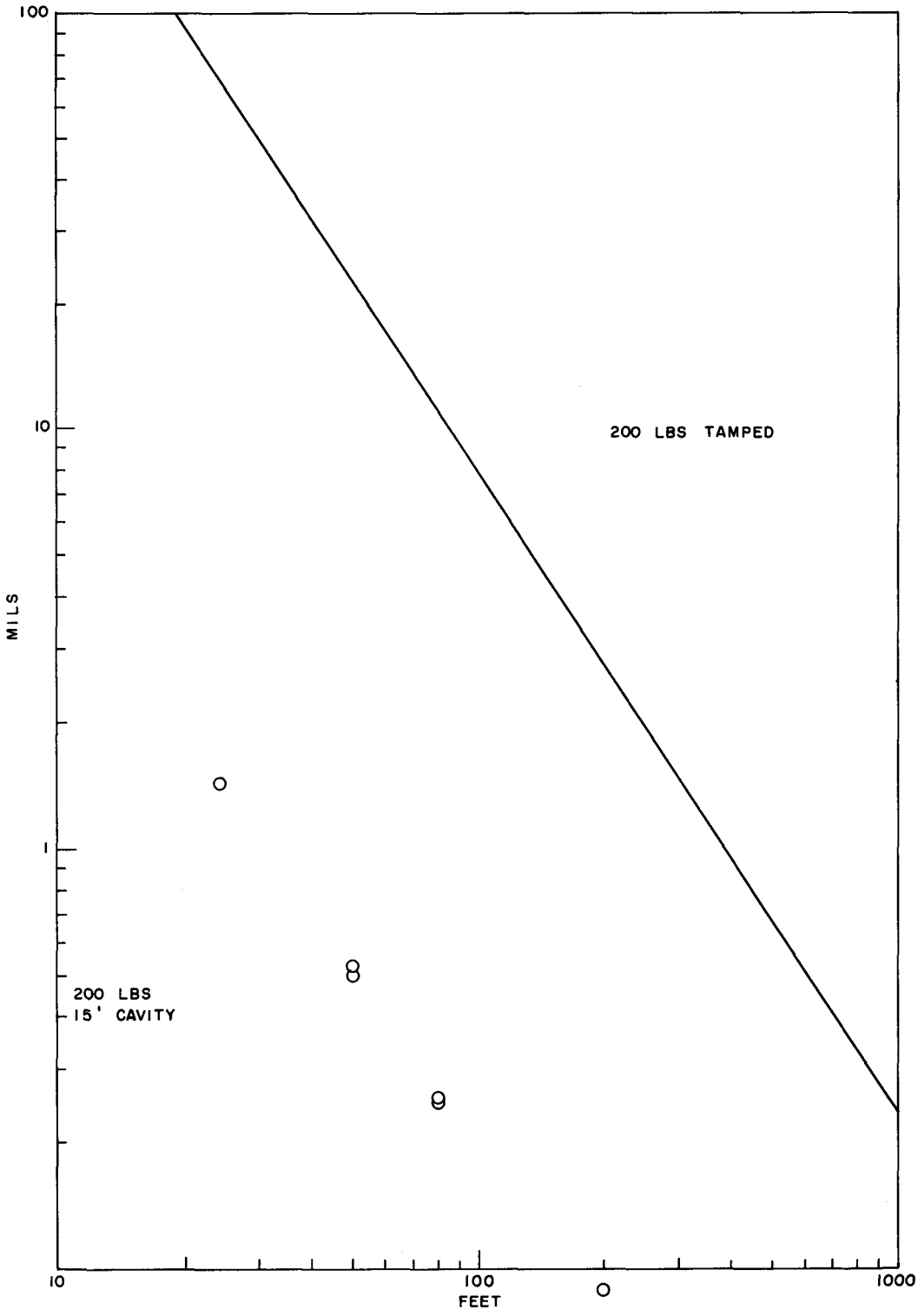

Fig. 3.12 Peak displacement versus distance, 200 lbs, 15-ft cavity

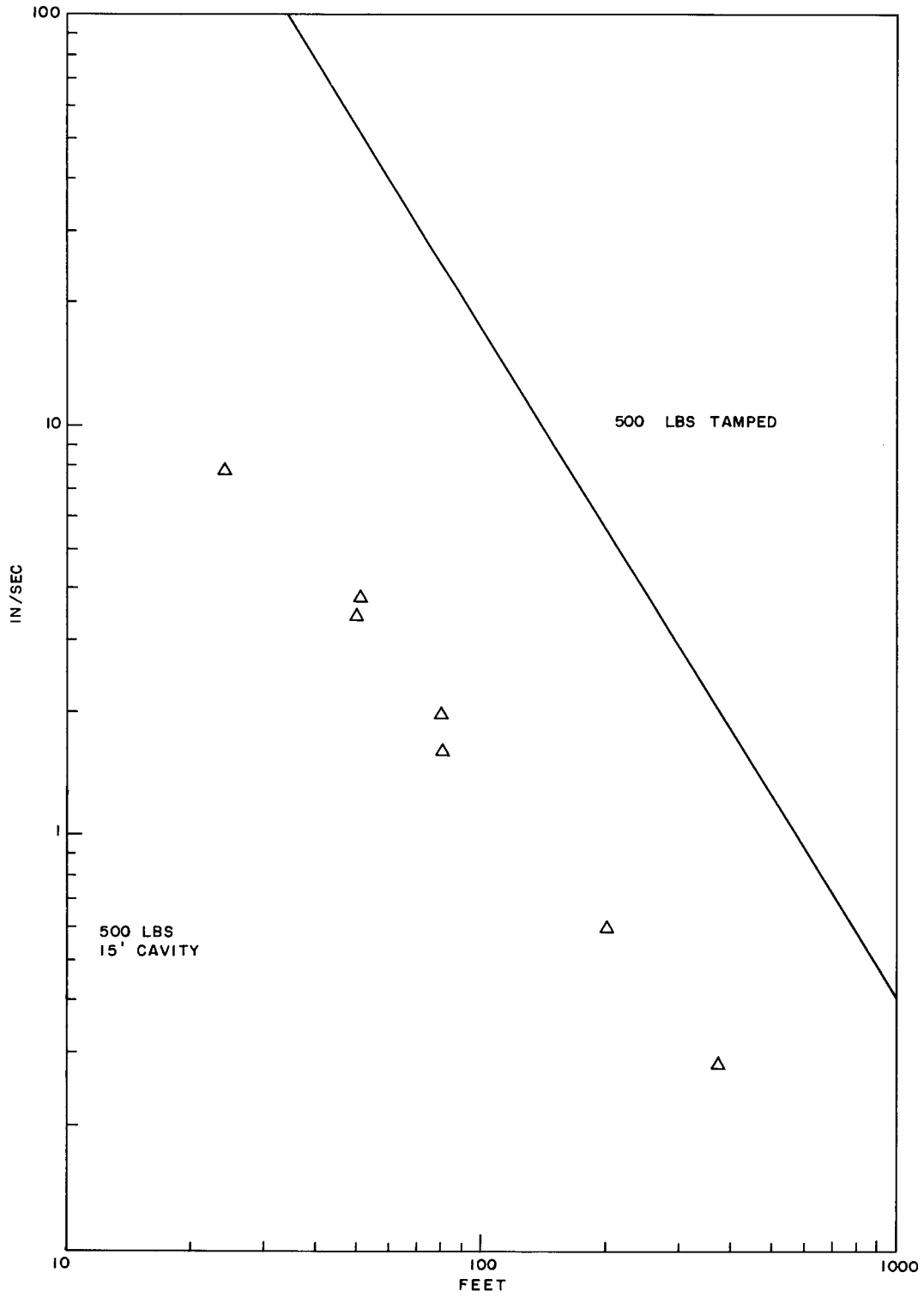

Fig. 3.13 Peak particle velocities versus distance, 500 lbs, 15-ft cavity

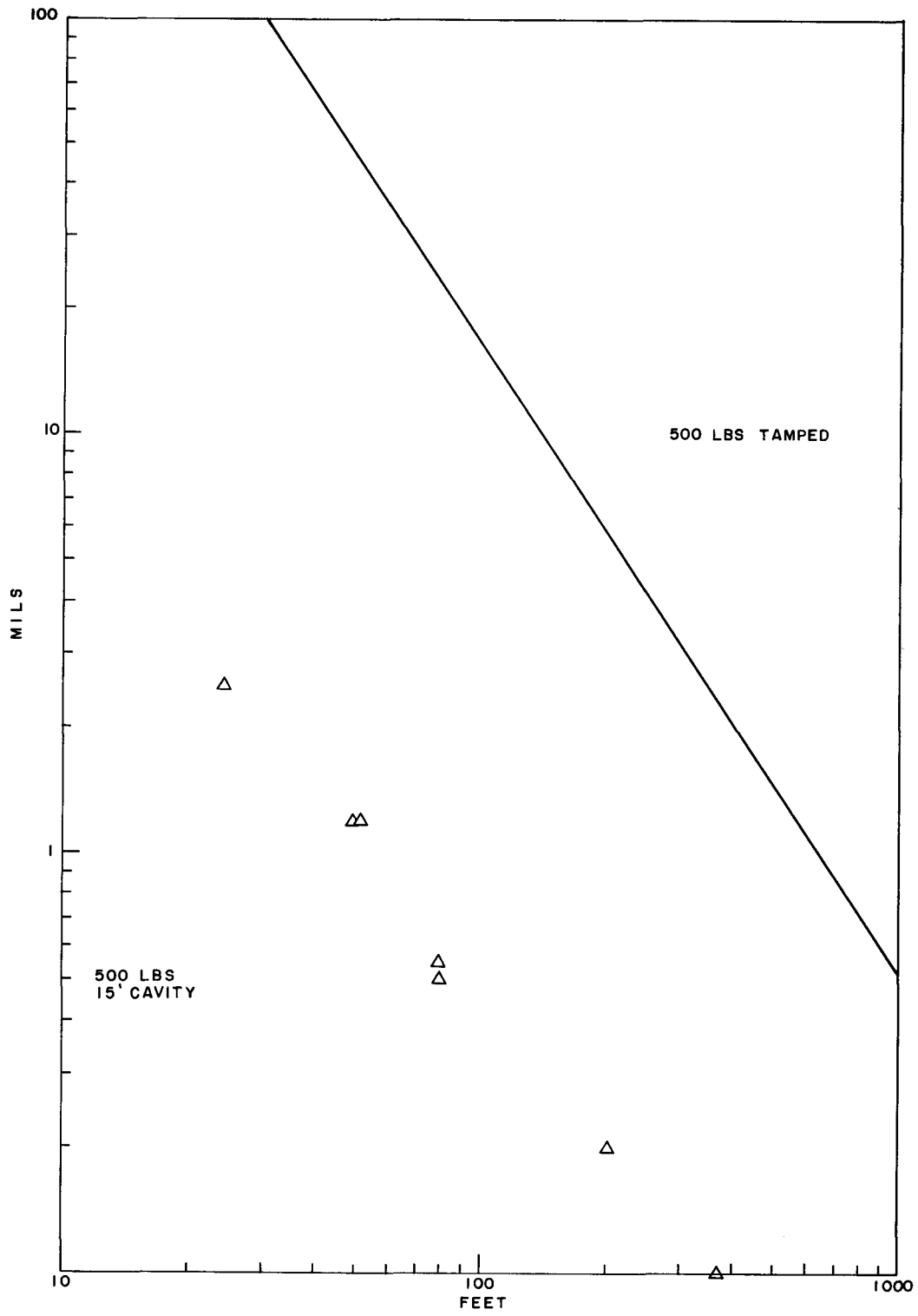

Fig. 3.14 Peak displacement versus distance, 500 lbs, 15-ft cavity

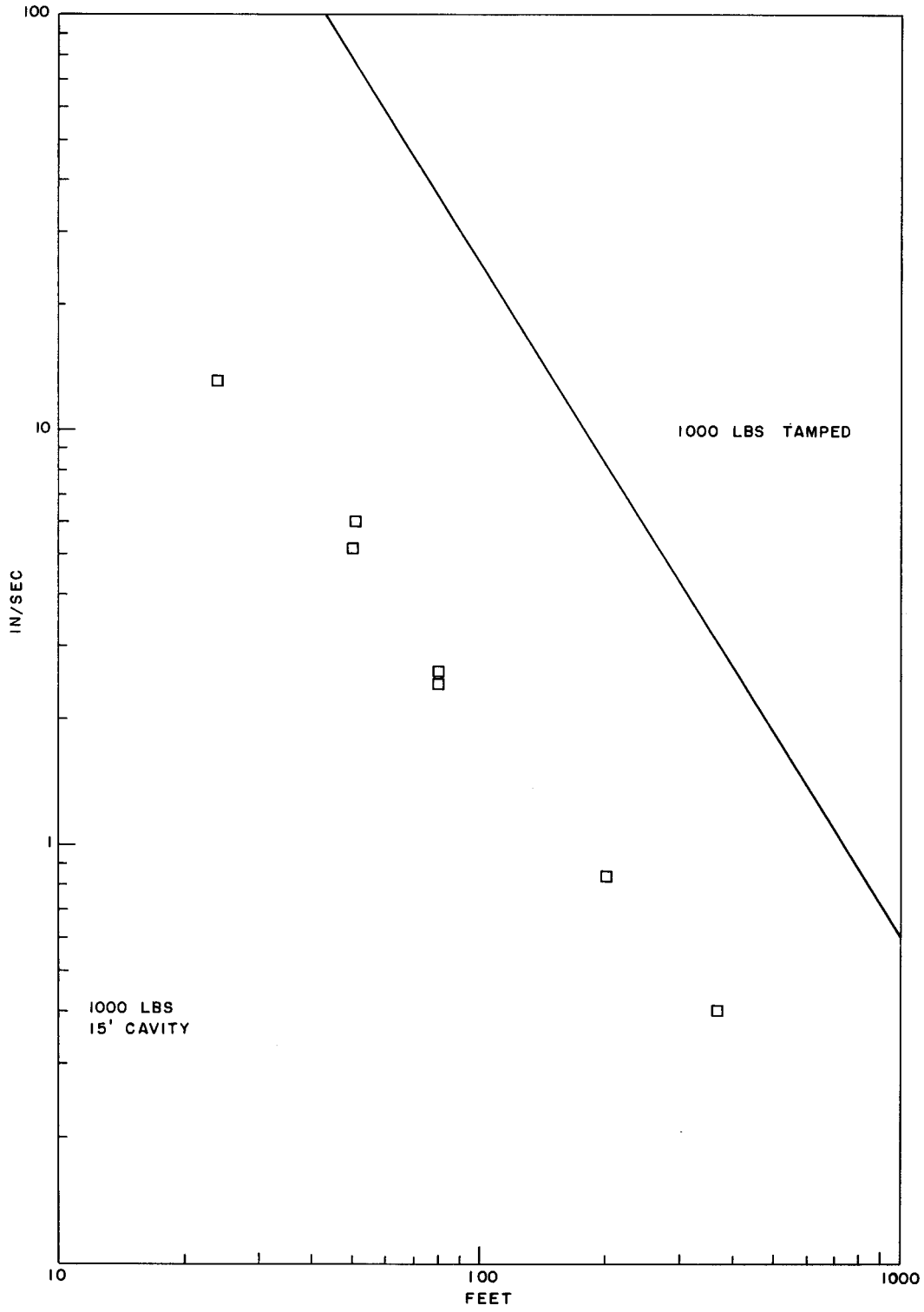

Fig. 3.15 Peak particle velocities versus distance, 1000 lbs, 15-ft cavity

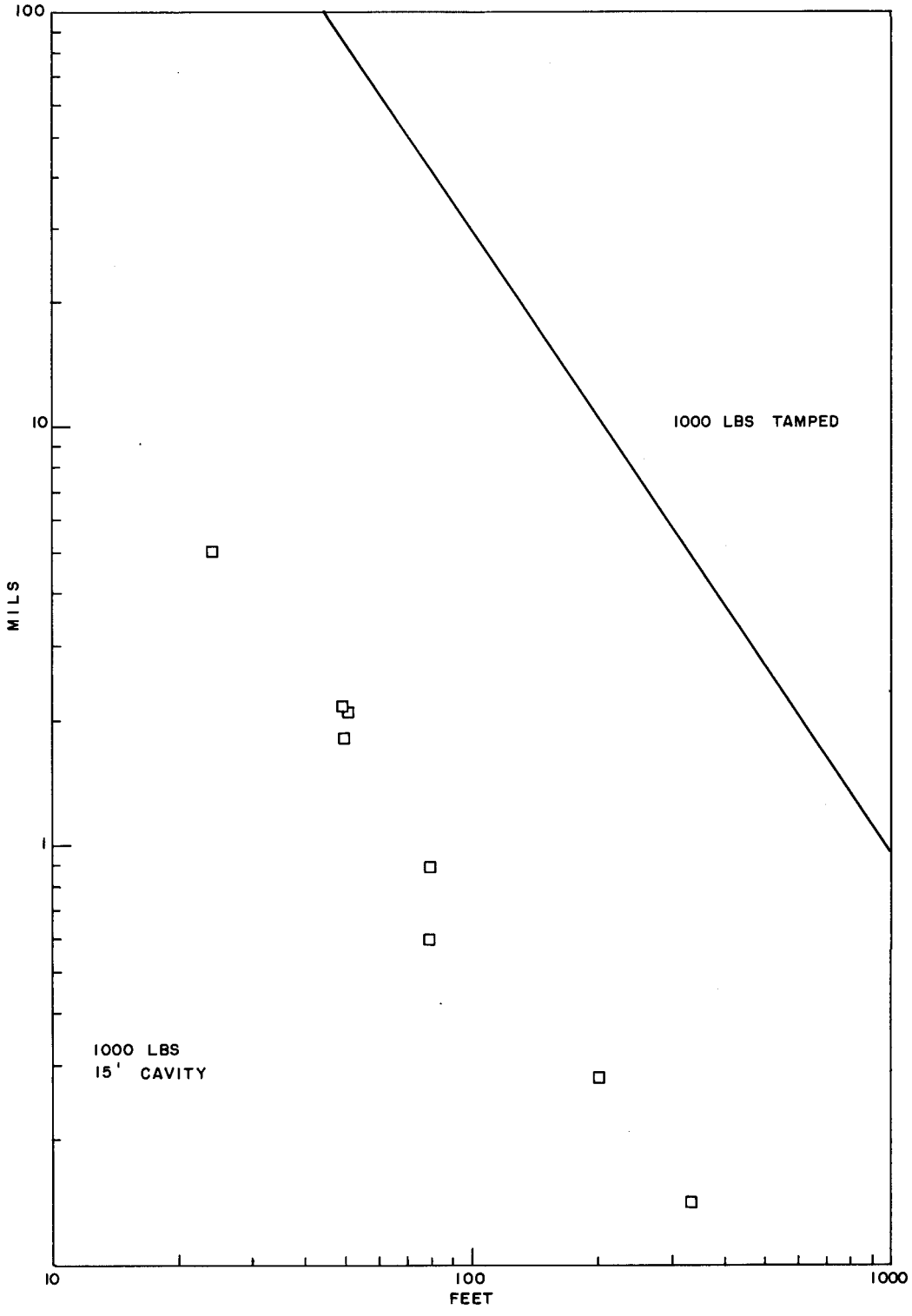

Fig. 3.16 Peak displacement versus distance, 1000 lbs, 15-ft cavity

Differences in the frequencies apparent in signals from tamped and cavity explosions may be inferred qualitatively from inspection of comparative velocity-time recordings. Copies of actual recordings of velocity versus time which were made by oscillograph recording on film are reproduced in the following figures:

Figure 3.17 Particle Velocities versus Time, 200 pounds, decoupled, 15-foot cavity

Figure 3.18 Particle Velocities versus Time, 200 pounds, coupled

Figure 3.19 Particle Velocities versus Time, 500 pounds, decoupled, 15-foot cavity

Figure 3.20 Particle Velocities versus Time, 500 pounds, coupled

Figure 3.21 Particle Velocities versus Time, 1000 pounds, decoupled, 15-foot cavity

Figure 3.22 Particle Velocities versus Time, 1000 pounds, coupled

Figure 3.23 Particle Velocities versus Time, 1000 pounds, decoupled, 6-foot cavity

Figure 3.24 Particle Velocities versus Time, 1000 pounds, coupled

Notable for the coupled shots is the fact that rise time for the change in particle velocity is slow enough for the gage to follow the motion with some accuracy. Such is not the case for the decoupled shots. The high frequency to be seen on the recordings of velocities from decoupled explosions is caused by ringing of the canister containing the gages. The degree of ringing varies from gage to gage because of variation in precautions taken to avoid the ringing. This ringing can be filtered out in playing back data from magnetic-tape recordings, and indeed it is automatically done upon integration to give displacement. It is questionable whether actual peak-particle velocity is always recorded accurately for decoupled explosions. The inaccuracy involved can be guessed at by

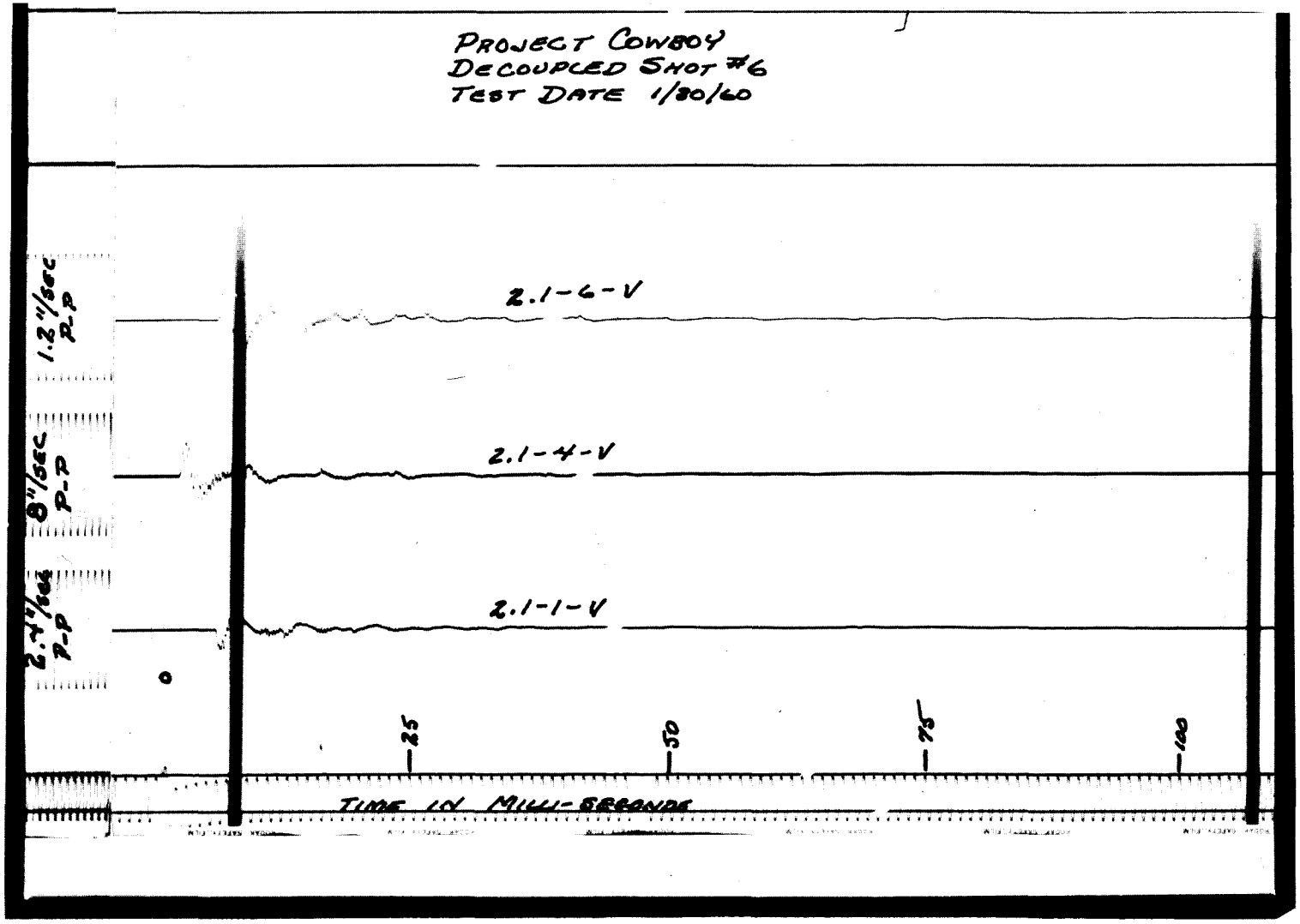

Fig. 3.17 Particle velocities versus time, 200 lbs decoupled 15 ft

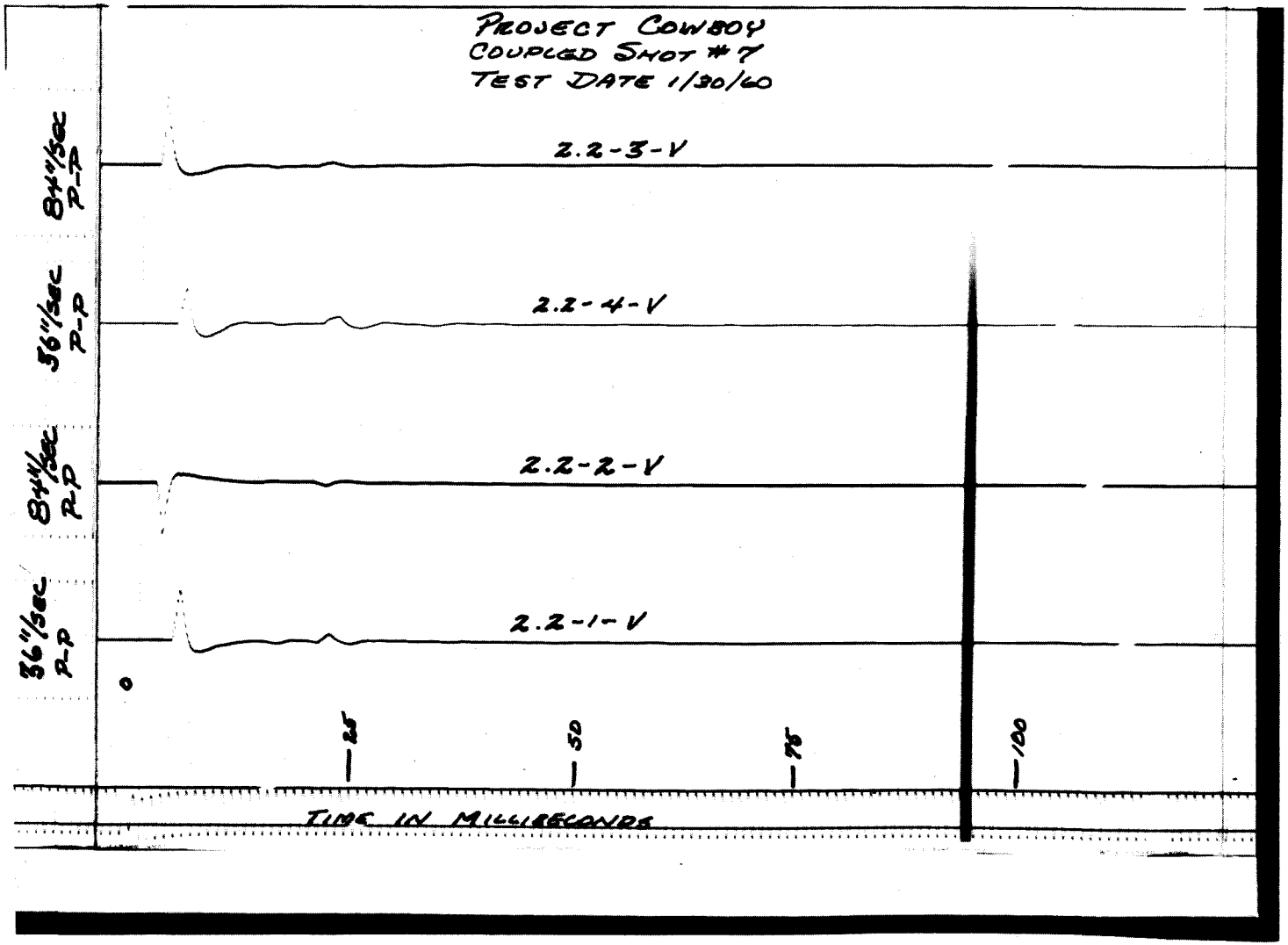

Fig. 3.18 Particle velocities versus time, 200 lbs coupled

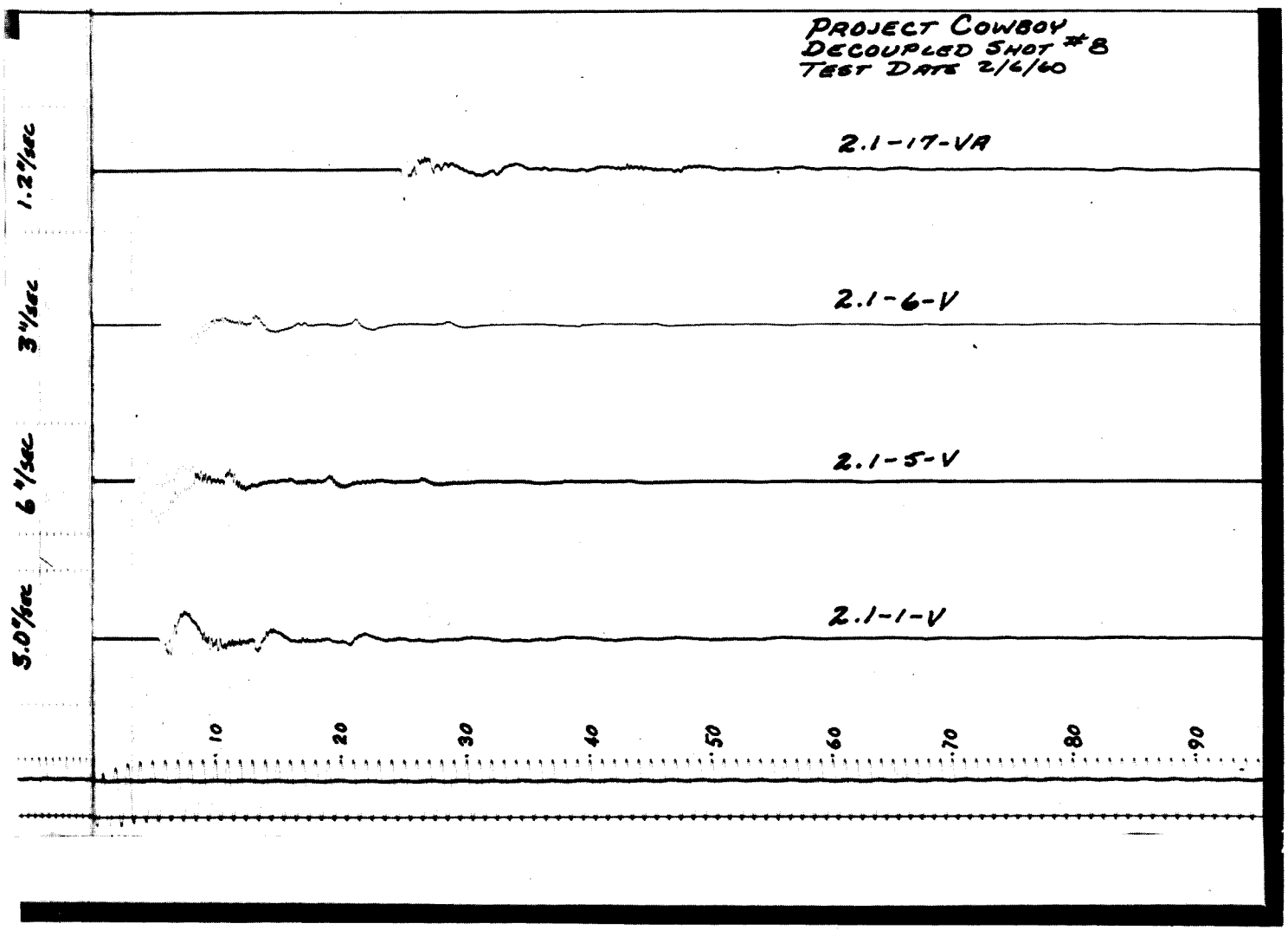

Fig. 3.19 Particle velocities versus time, 500 lbs decoupled 15 ft

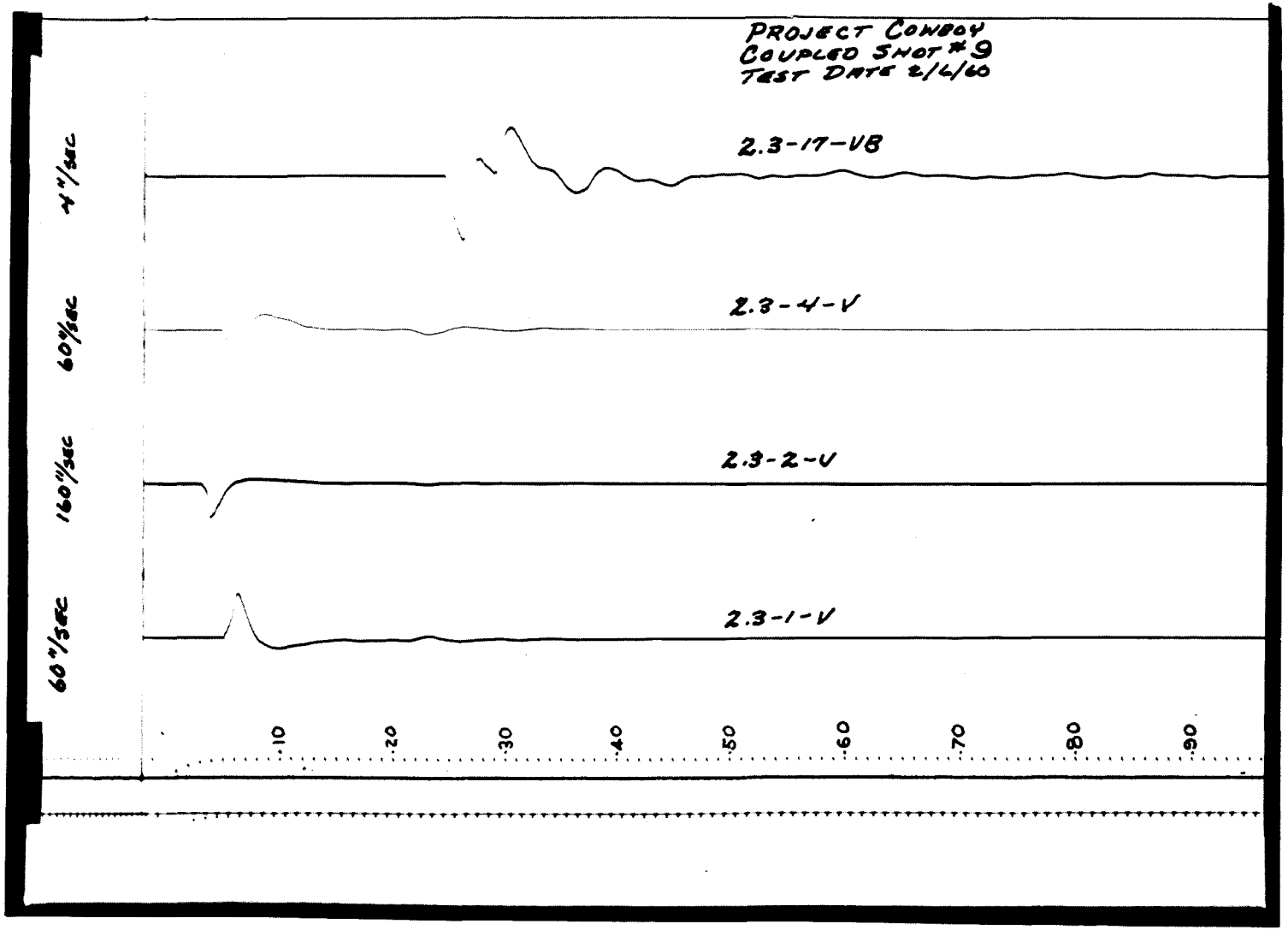

Fig. 3.20 Particle velocities versus time, 500 lbs coupled

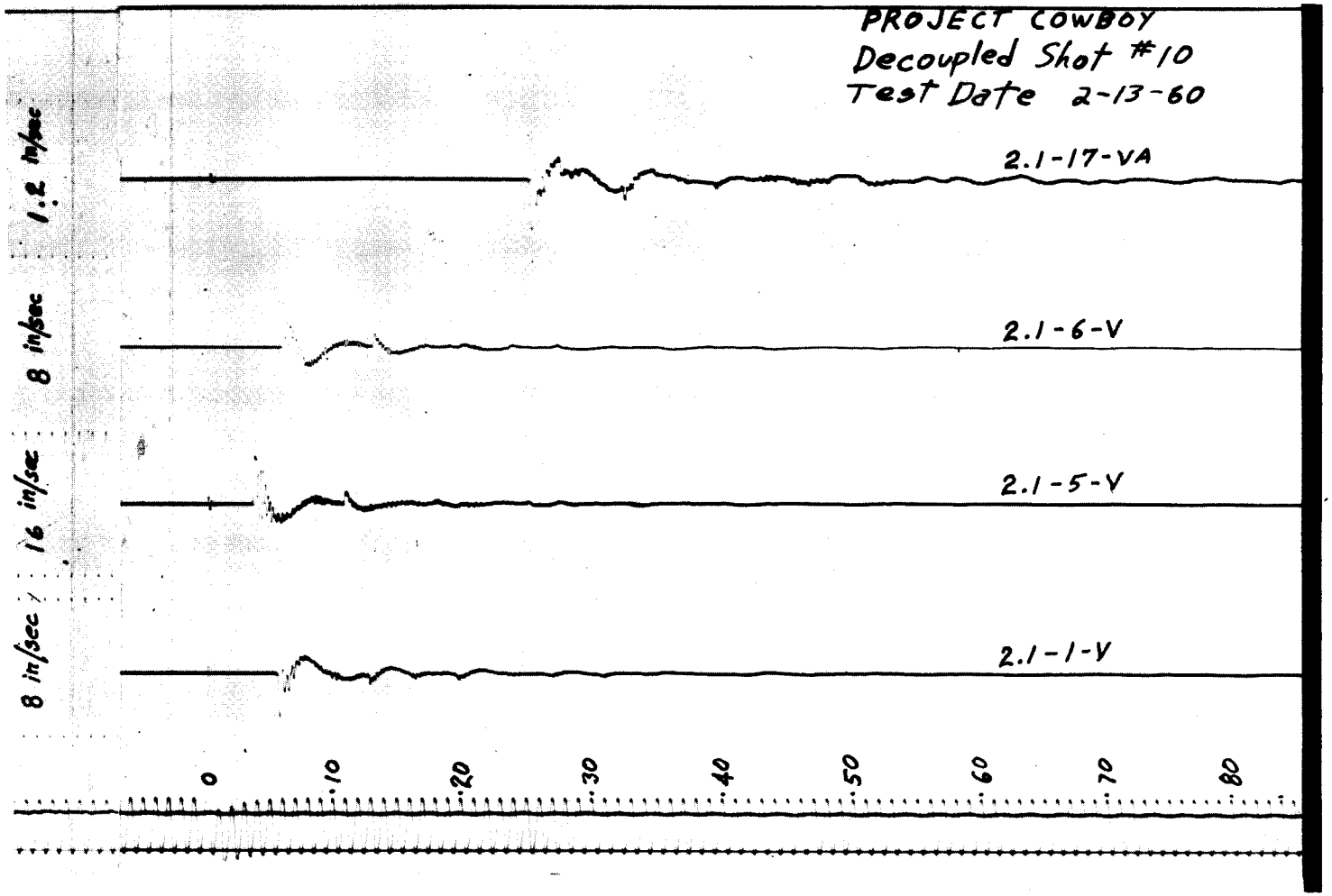

Fig. 3.21 Particle velocities versus time, 1000 lbs decoupled 15 ft

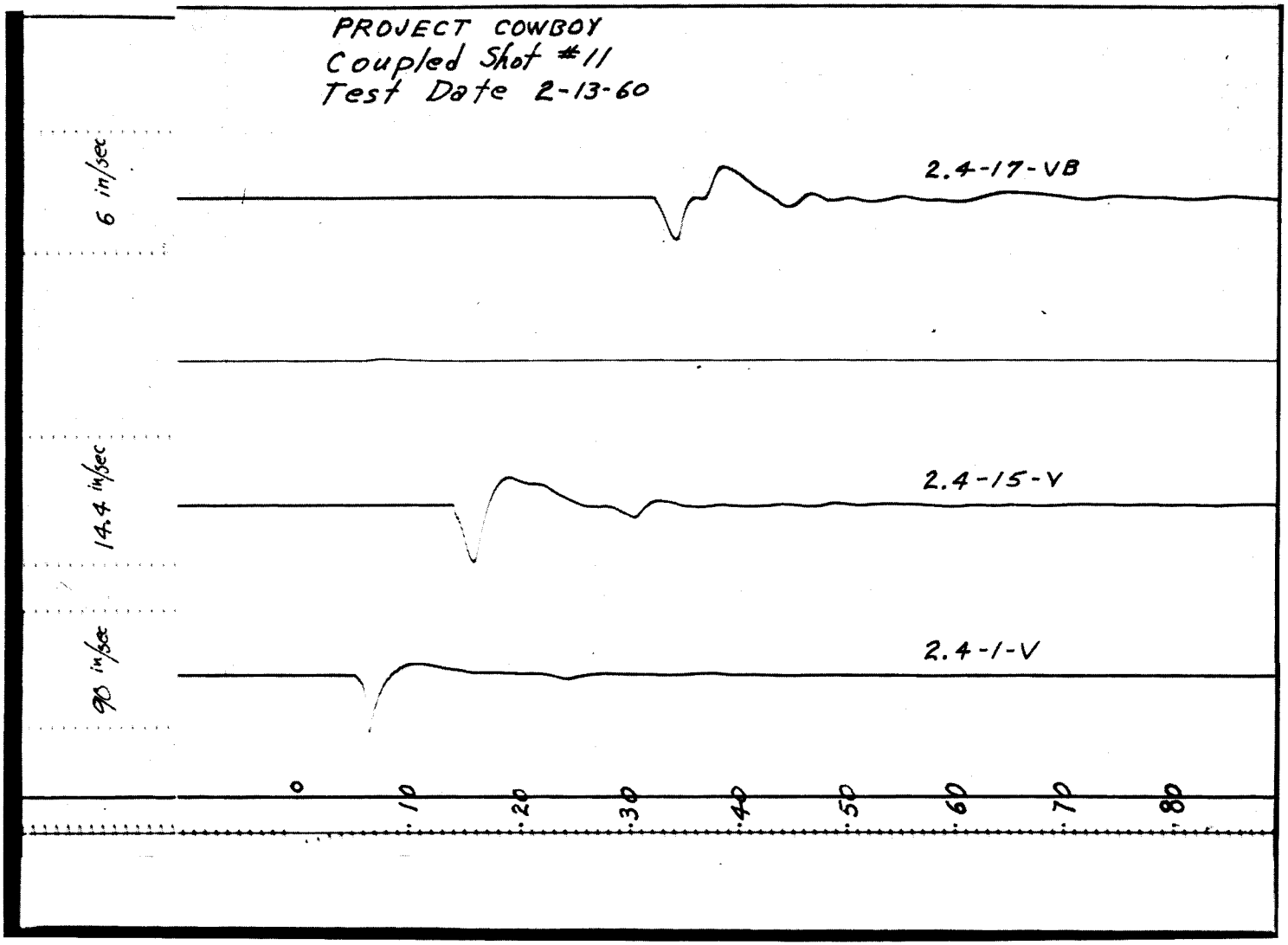

Fig. 3.22 Particle velocities versus time, 1000 lbs coupled

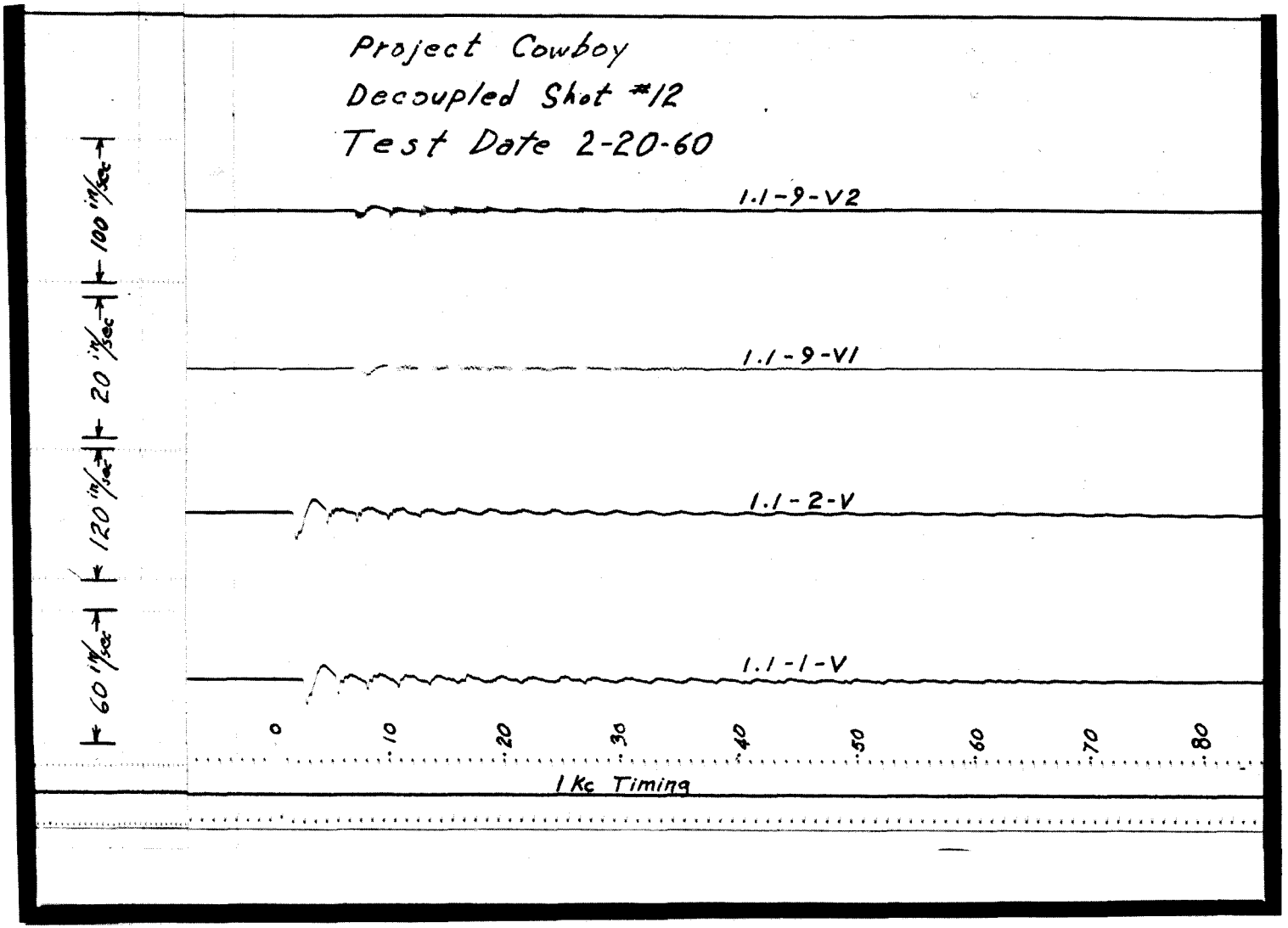

Fig. 3.23 Particle velocities versus time, 1000 lbs decoupled 6-ft cavity

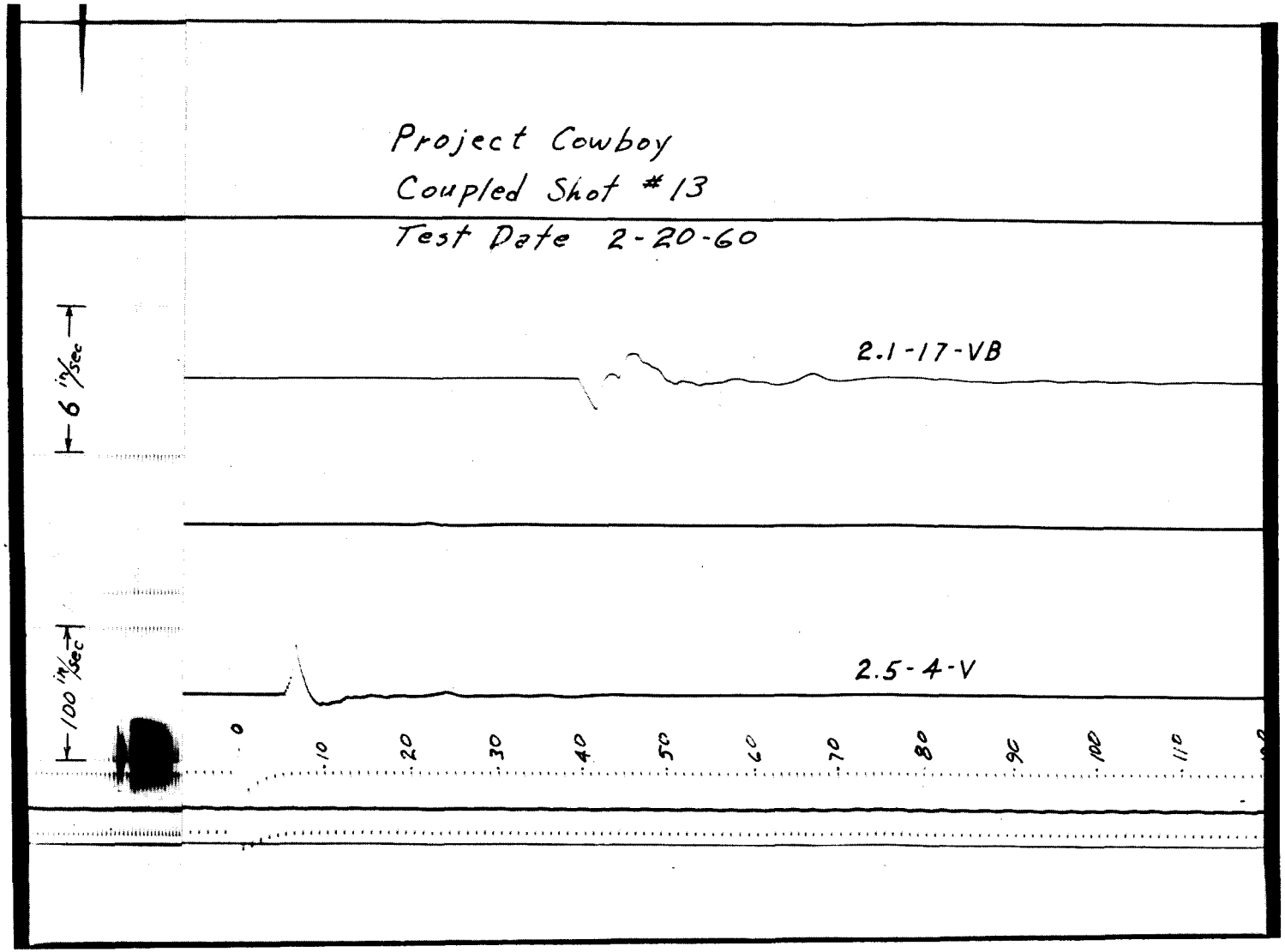

Fig. 3.24 Particle velocities versus time, 1000 lbs coupled

extrapolating back to arrival time of the shock front, if it is assumed that a step shock front existed. (See results of pressure-time measurements, Section 3.3.)

3.2 PERMANENT DISPLACEMENTS

The closest distance at which a good recording of velocity from a tamped shot was ob. ained was $6.28\ r/W^{1/3}$. The recording and integration by a network to give displacement versus time shown in Fig. 3.25 were obtained at 50.5 feet from a 500-pound tamped explosion. Since the integrating network cuts off low frequencies, displacement recording is only useful for measuring peak displacements.

Velocity-time recording was also measured point by point on a Telereader and integrated on a computer to produce displacement versus time, as illustrated in Fig. 3.26. Negative displacement at long times merely reflects the difficulty of reading true velocity zero. A low-frequency signal of amplitude around 10 mils must, however, exist. The Fourier transform for velocity versus time is shown in Fig. 3.27.

Another method of obtaining permanent displacement is to doubly integrate accelerations. Even more serious difficulties are encountered because the ratio between high- and low-frequency amplitudes for acceleration is even greater than for velocities. However, a trick to minimize these difficulties is possible: one can use an accelerometer of high sensitivity to low-frequency accelerations with a low resonant frequency so that higher frequencies are rejected at 12 db per octave. The high-frequency signal may still be the largest signal recorded if the resonant frequency of the accelerometer is not low enough. Further rejection of the high-frequency

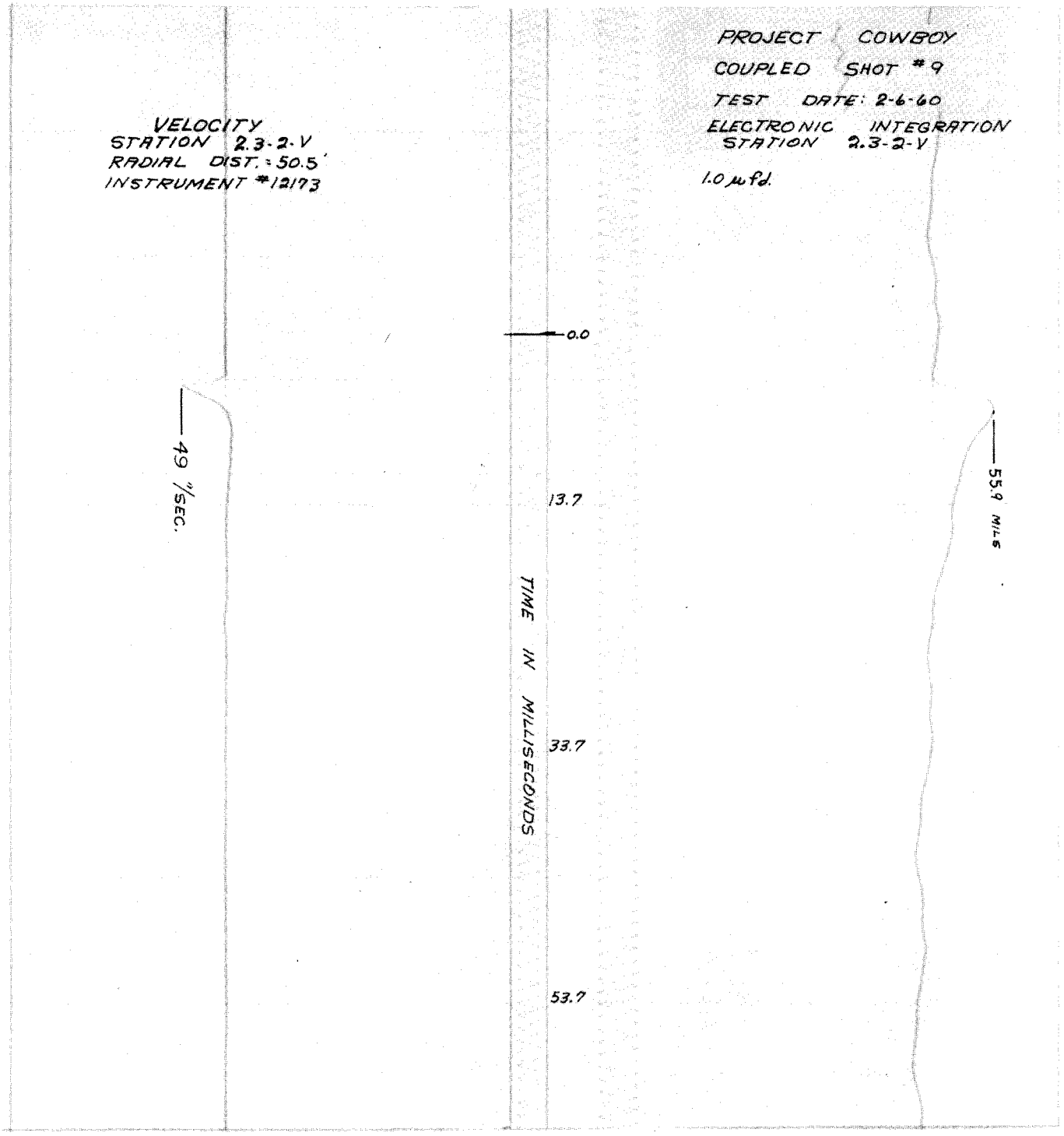

Fig. 3.25 Particle velocity and displacement versus time

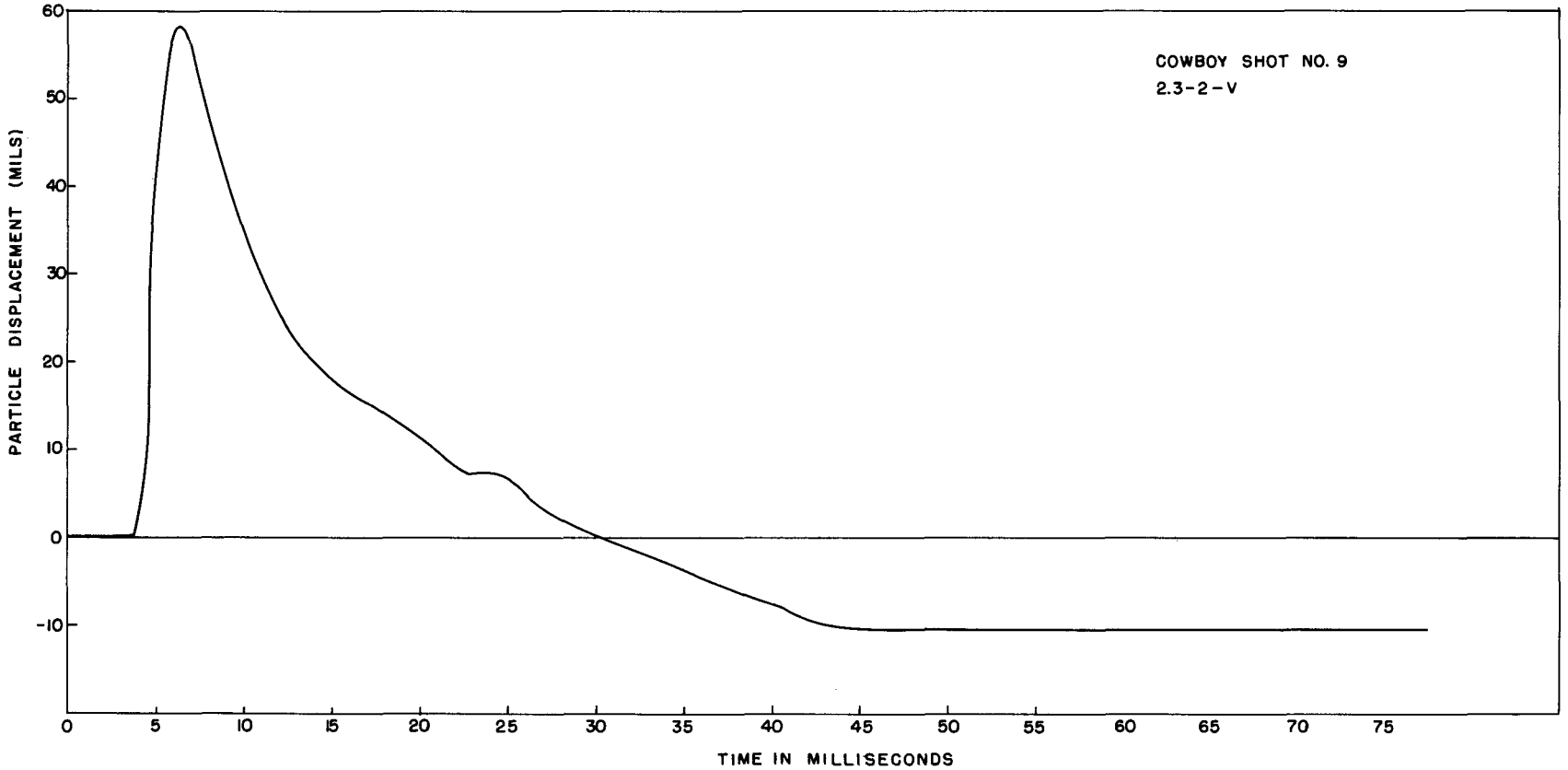

Fig. 3.26 Particle displacement versus time

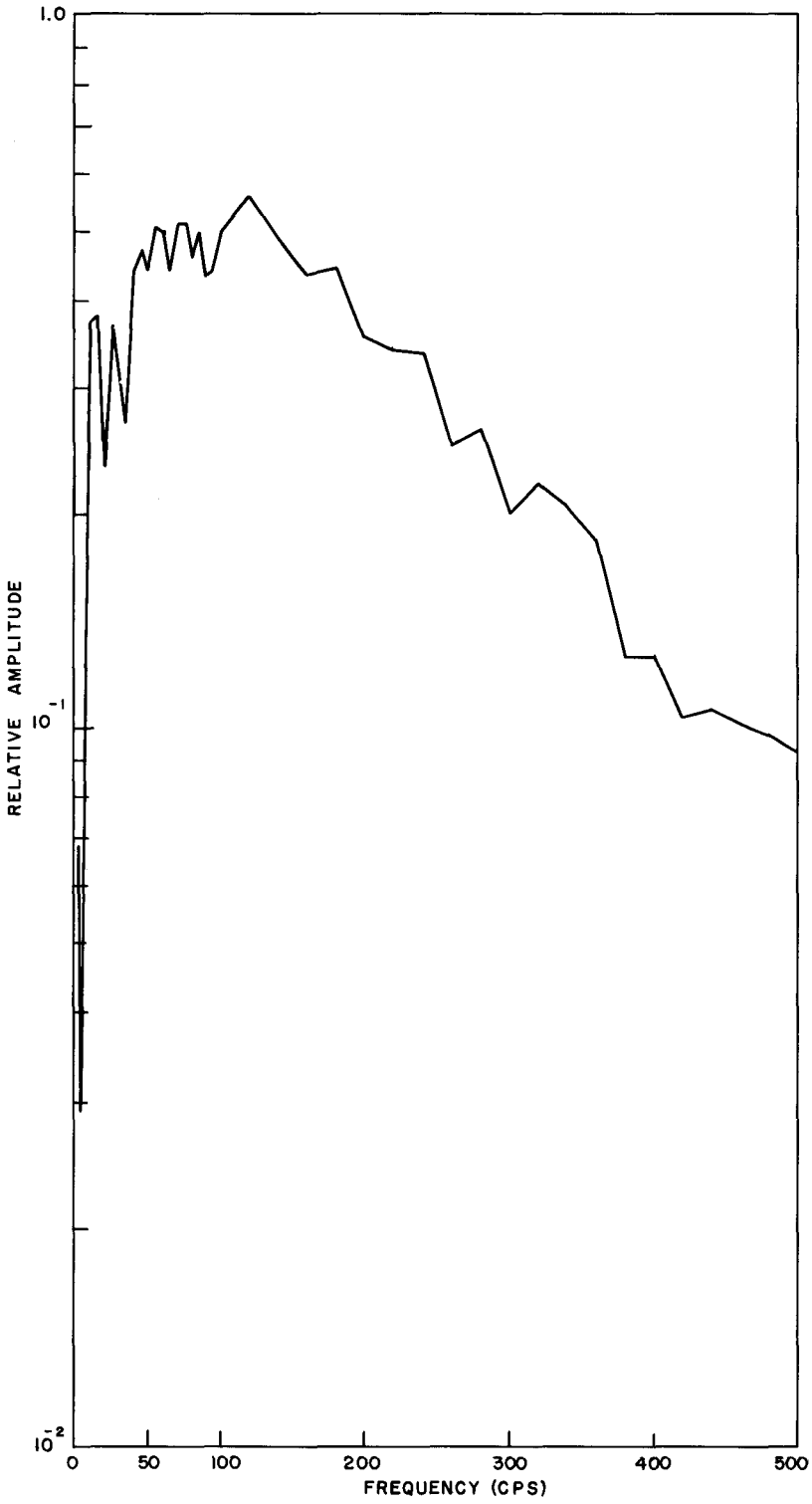

Fig. 3.27 Fourier transform

information is possible by playing back the tape record through successive low-pass filters. When this technique is applied, the records obtained at low frequencies amount to about a cycle and a half of information at the frequency of the low-pass filter. The amplitude of the low-pass signal becomes smaller in proportion to the square of the upper frequency limit of the low-pass filter as lower frequency, low-pass filtering is applied. The amplitude of the computed displacement, acceleration x (information frequency),^{2} remains about constant. This computed displacement presumably then represents the amplitude of the actual permanent displacement.

The permanent displacement computed in this manner at a distance of 80.6 feet from the 200-pound coupled Shot No. 7 turned out to be 1 mil. The peak transient displacement at the same position was 8 mils (integration of velocity-time record).

This experiment was also conducted at distances of 52.2 and 80.9 feet from the 1000-pound coupled Shot No. 13. The gage at 52.2 feet was damaged by a much larger acceleration than it was designed to take. The undamaged gage at 80.9 feet indicates that the permanent displacement was between 10 and 14 mils. This result is roughly consistent with the result from the 200-pound shot. Integration of the velocity-time records from the same position (Shot No. 13, 80.9-foot radius) illustrated in Fig. 3.28 gives a permanent displacement of 8 mils after a transient peak of 42 mils. The record from another gage (Shot No. 11, 77.5-foot radius) shown in Fig. 3.29 gives a negative permanent displacement. About all that can be concluded is that a transient displacement near 20 cps of peak-to-peak amplitude of 10 mils did occur.

As another check on the maximum possible value of permanent displacement from coupled shots, nearly all of the velocity-time records were played

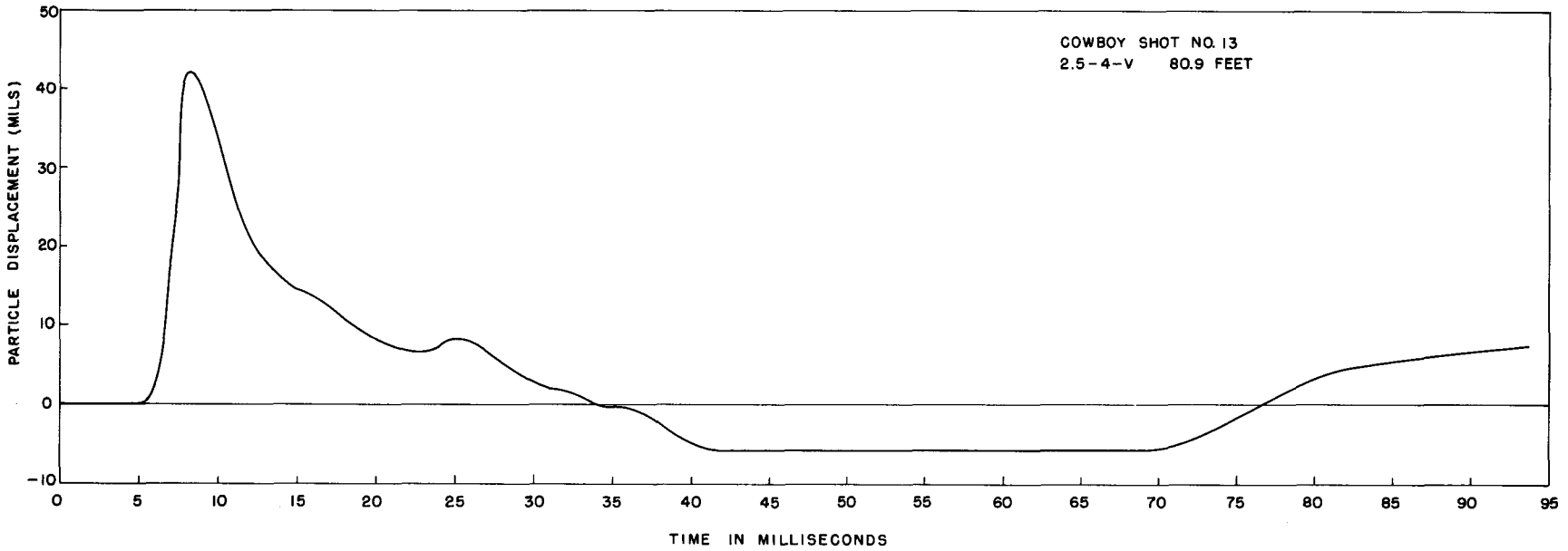

Fig. 3.28 Particle displacement versus time, 80.9 ft

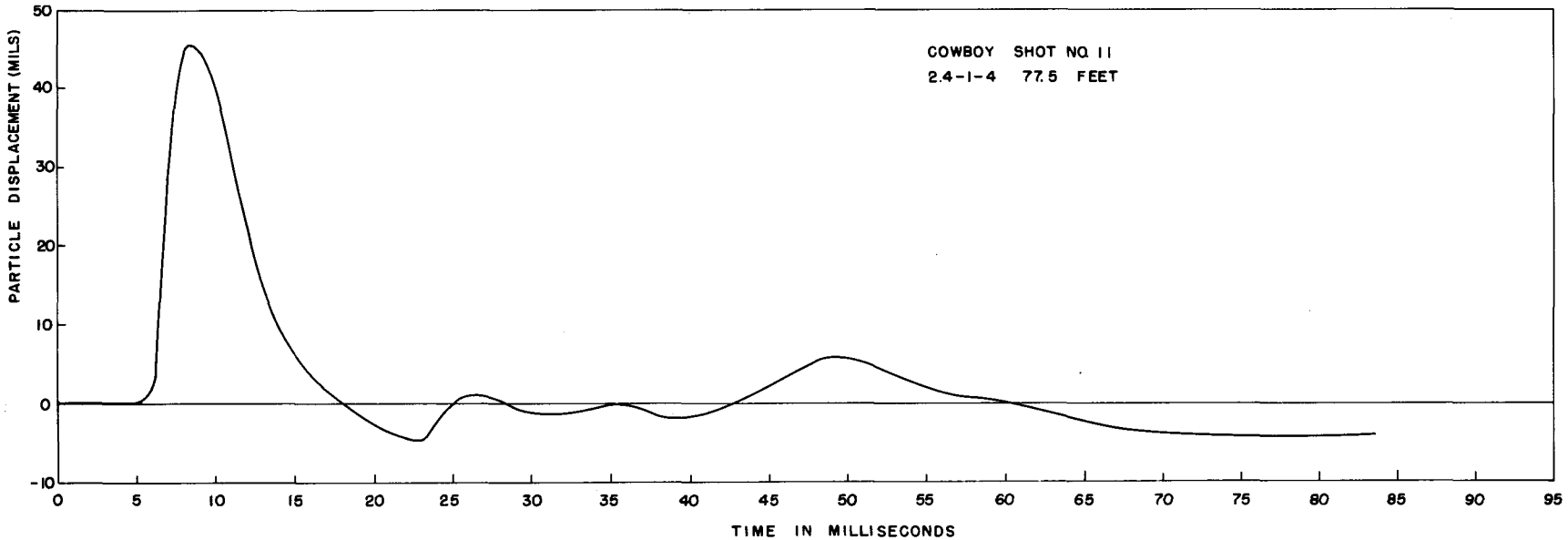

Fig. 3.29 Particle displacement versus time, 77.5 ft

back through 40 cps and 10 cps low-pass filters with the idea that more low-frequency signal-to-noise ratio could be preserved in this way than in either hand or electronic integration. Most importantly, the low-pass filtering eliminates error in determing velocity zero which always plagues hand integration. As with the technique described for the special accelerometer, low-frequency velocity was integrated according to the signal information frequency passed. When this was done, displacement amplitude was always still decreasing with low-pass filtering frequency until the signal disappeared in the noise.

If peak displacement were not so much larger than permanent displacement, the integration could give more accurate permanent displacements. Evidently our instruments were always in the region of elastic behavior of the salt, and the mass "inductive" motion was too small for us to measure, even from the tamped explosions. This point is discussed further in Chapter 4.

Since it became clear almost at once in the Cowboy experiments that peak displacements were high compared to permanent displacements at the distances of observation, an effort was made to design and place a displacement gage. The first model was placed at 49.9 feet from the center of the 15-foot radius cavity. Records from this displacement gage were obtained on the 500- and 1000-pound cavity Shots 8 and 10 (Figs. 4.3 and 4.4, Section 4.3). The permanent displacement on Shot 8, inferred from this gage at 90 milliseconds after shock arrival, was less than 3 percent of the peak displacement of 1.2 mils. Insufficient accuracy was obtained to read the very small permanent displacement. Peak displacements checked with integrated velocities fairly well (see Table 3.3).

Displacement gage records provide evidence of the natural oscillation of the cavity (see Section 5.3).

3.3 PRESSURE-TIME HISTORY IN THE CAVITY

Since the pressure on the cavity wall from an explosion is not truly a step function, actual pressure-time histories in the cavity were desired over both short- and long-time intervals. Pressure gages were placed near the door and at angles of 45 and 90 degrees from the door. A slow-response pressure gage was also placed near the door to measure cavity pressure at long times after the explosion.

The best illustration of pressure versus time in the cavity is provided by results from Shot No. 10. Data recorded by 3 gages in the three positions are illustrated in Fig. 3.30 for 1000 pounds of Pelletol in the 15-foot radius cavity. The first pressure pulse had an amplitude near 900 psi, the second about 300 psi, and the third about 100 psi. The gas pressure continued to oscillate for some time. Figure 3.31 illustrates the cavity pressure at long times for the same explosion. This gage was purposely arranged to have a long fill time so that it would not record peak transient pressures. The cavity pressure at 100 milliseconds is 90 psi, or about one-tenth of the initial peak pressure.

Comparative peak pressures and pressures at 100 milliseconds after zero time for explosions in the 15-foot cavity are listed in the following table.

Pressures in 15-Foot Cavity

W (lbs)	Shot No.	Peak pressure (psi)	Pressure at 100 msec (psi)	$p = \frac{(\gamma - 1)W}{\frac{4}{3}\pi 15^3}$ (psi)
198	5	~300	22	28
477	8	500	44	67
954	10	900	92	135

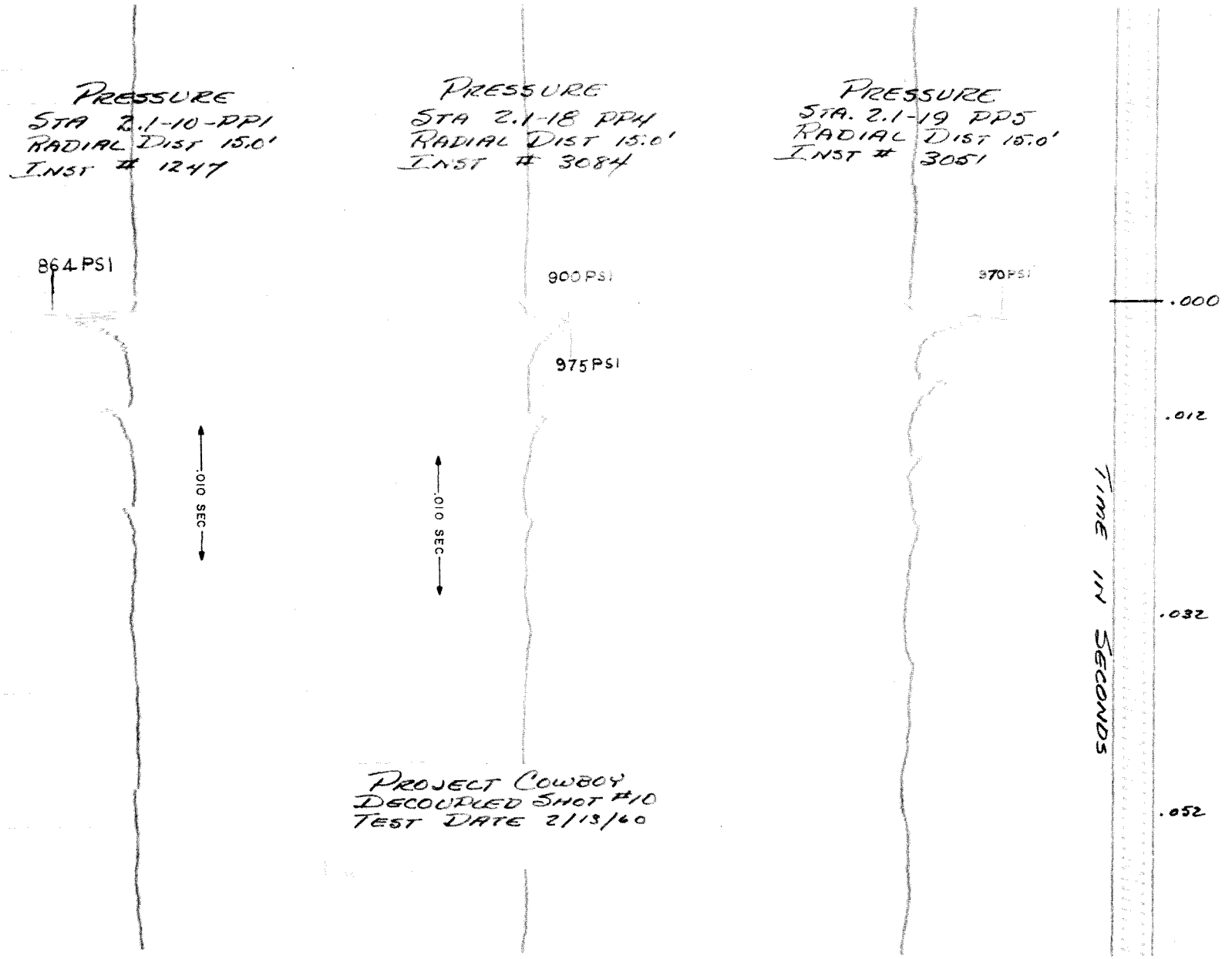

Fig. 3.30 Pressure versus time, 1000 lbs, 15-ft radius cavity

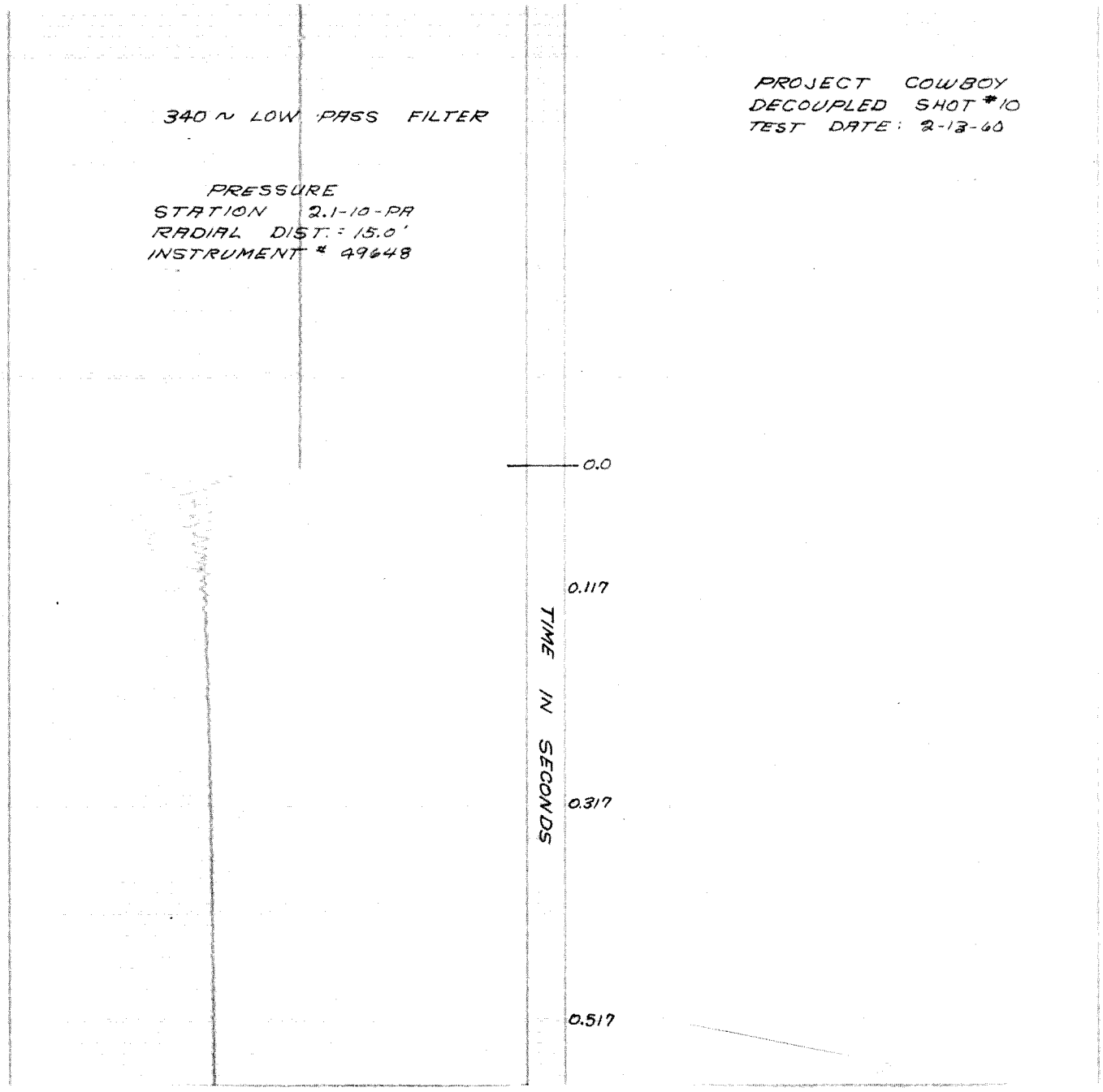

Fig. 3.31 Cavity pressure at long times

In the above table, $\gamma = 1.2$ has been used because the cavity was evacuated and the energy release of Pelletol was assumed to be 1000 cal/gm. If the pressure at 100 milliseconds is extrapolated back to zero time, and one ignores peak pressure, numbers closer to calculated pressures are obtained.

Although an attempt was made to measure peak pressure in the 6-foot cavity and results are only of qualitative significance, they are listed below.

Pressures in 6-Foot Cavity

W (lbs)	Shot No.	Peak pressure (psi)	Late pressure (psi)
20	2	200	26
100	3	--	155

3.4 THERMOCOUPLE MEASUREMENTS IN THE CAVITIES

Each cavity was instrumented with a thermocouple. The thermocouple, of course, could not follow the gas temperature changes, but could serve to give a measure of the temperature near the wall after a few seconds.

The peak temperature observed and the temperatures 3 minutes after the explosion are listed below. Ambient temperature was 100 degrees F.

Thermocouple Temperature Measurements

Shot No.	W (lbs)	T peak (degrees F)	T at 3 minutes (degrees F)
2	20	280	125
3	100	1025	270
12	1000	900	260
14	2000	thermocouple shorted near zero time	
5	200	no record	no record
6	200	248	140
8	500	325	150
10	1000	460	230

Temperature changes require subtraction of 100 from the above numbers.

3.5 PLUG AND LINER MOTION

Creation of 6- and 15-foot radius cavities required access drifts which had to be lined and plugged. Steel liners, 40 feet in length, were cemented to the massive salt walls. The small 2-foot-diameter opening to each cavity was sealed with a steel plug, which in turn was backed up by a series of tightly fitting plugs.

After the 200-pound experiments, some of the LRL theoretical staff suggested that we should know motion of the plug and liner in case such motion was large compared to the motion of the salt. A velocity gage was therefore placed at a free surface at the end of the liner 40 feet from the center of the cavity. Peak velocities and displacements observed are listed below in comparison with the interpolated motion in the salt, taken from Figs. 3.13 through 3.16. Division of liner motion by 2 is indicated to take account of the free surface.

Liner Motion, 15-Foot Cavity

W (lbs)	Peak velocity (in/sec) Liner	Salt	Peak displacement (mils) Liner	Salt
500	$\frac{9.2}{2}$	4.6	$\frac{3.5}{2}$	1.5
1000	$\frac{10.6}{2}$	7	$\frac{6.8}{2}$	2.8

The liner of the plug for the 15-foot cavity evidently carried the load satisfactorily.

Both plug and liner were instrumented for the 1000- and 2000-pound explosions in the 6-foot sphere at a distance of 30.7 feet from the center of the cavity.

W (lbs)	Peak velocity (in/sec) Plug	Liner	Salt	Peak displacement (mils) Plug	Liner	Salt
1000	$\frac{23.3}{2}$	$\frac{51.4}{2}$	16	$\frac{82}{2}$	$\frac{38.5}{2}$	11
2000	> 65	$> \frac{100}{2}$	33	--	> 200	26

Actually, the plug failed on the 2000-pound shot. Until cable breakage at about 200 milliseconds, the plug had not moved far. From postshot observations, it eventually moved a good many feet.

3.6 ACCELERATIONS AT 67 $r/W^{1/3}$

ALO/OTO and the Bureau of Mines requested acceleration measurements at a distance of 67 $r/W^{1/3}$ from all tamped shots in order to predict what

accelerations would be observed at this distance from a 10,000-pound tamped explosion. Accelerometers were placed in the wall and floor of the drift leading from the main shaft to the Cowboy experimental area. The data were reported to the above agencies. Observations for decoupled shots are reported below:

Decoupled Shot Observations

W (lbs)	Shot	Type	Distance (feet)	Wall acceleration (g's)	Floor acceleration (g's)
477	8	15-foot cavity	666	0.02	0.05
500	9	tamped	540	0.8	1.1
954	10	15-foot cavity	690	0.09	0.12
1000	11	tamped	658	0.92	0.85
929	12	6-foot cavity	645	0.19	0.22
1000	13	tamped	667	1.1	0.87
1903	14	6-foot cavity	855	0.4	0.4
933	15	tamped	449	2.5	1.5

The acceleration at 67 $r/W^{1/3}$ from a tamped explosion, as seen by a gage mounted near the surface of the floor or wall, is about 1 g as observed in the Carey salt mine.

It is noteworthy that the decoupling near 670 feet from Shots 12 and 13 was between 4 and 5 to 1.

3.7 ACCELERATIONS WITHIN 80 FEET

Because the velocity meters worked well for those experiments in salt, acceleration data can essentially be ignored. It is fortunate that the velocity meters worked well, since the accelerometers either did not function properly or the high-frequency response was inadequate.

A considerable effort was made to employ piezoelectric accelerometers to provide adequate frequency response. In almost all records from piezoelectric accelerometers either the preamplifier functioned improperly, or the gage "rang" at both its fundamental frequency and the canister-ringing frequency, so that interpretation of acceleration was very doubtful. Possibly useful information could be obtained by detailed analysis, but it was decided to concentrate attention on analysis of the velocity data.

Variable-reluctance accelerometers performed satisfactorily, taking into consideration the limitation in frequency response. In order to obtain adequate frequency response with variable-reluctance accelerometers for Cowboy yields in salt, one must choose an accelerometer that is capable of measuring many more g's than will actually occur. We relied upon piezoelectric accelerometers for high-frequency response and variable reluctance units for low-frequency signals if they occurred.

Recordings from four variable-reluctance accelerometers have been doubly integrated to obtain displacement versus time. The first integration to give velocity yields a result which is in error because the velocity does not return to zero. We applied the customary arbitrary correction to bring the velocity back to zero. The trouble with the method is that the possible error in the displacement is large and difficult to evaluate.

Corrected velocity-time data are shown in Fig. 3.32 for the following integrated accelerometer recordings:

Shot No.	Yield (lbs)	Station	Distance (feet)
11	1000	2.4-2-AR	49.8
11	1000	2.4-3-AR	50.2
13	1000	2.5-3-AR	52.2
13	1000	2.5-4-AR	80.9

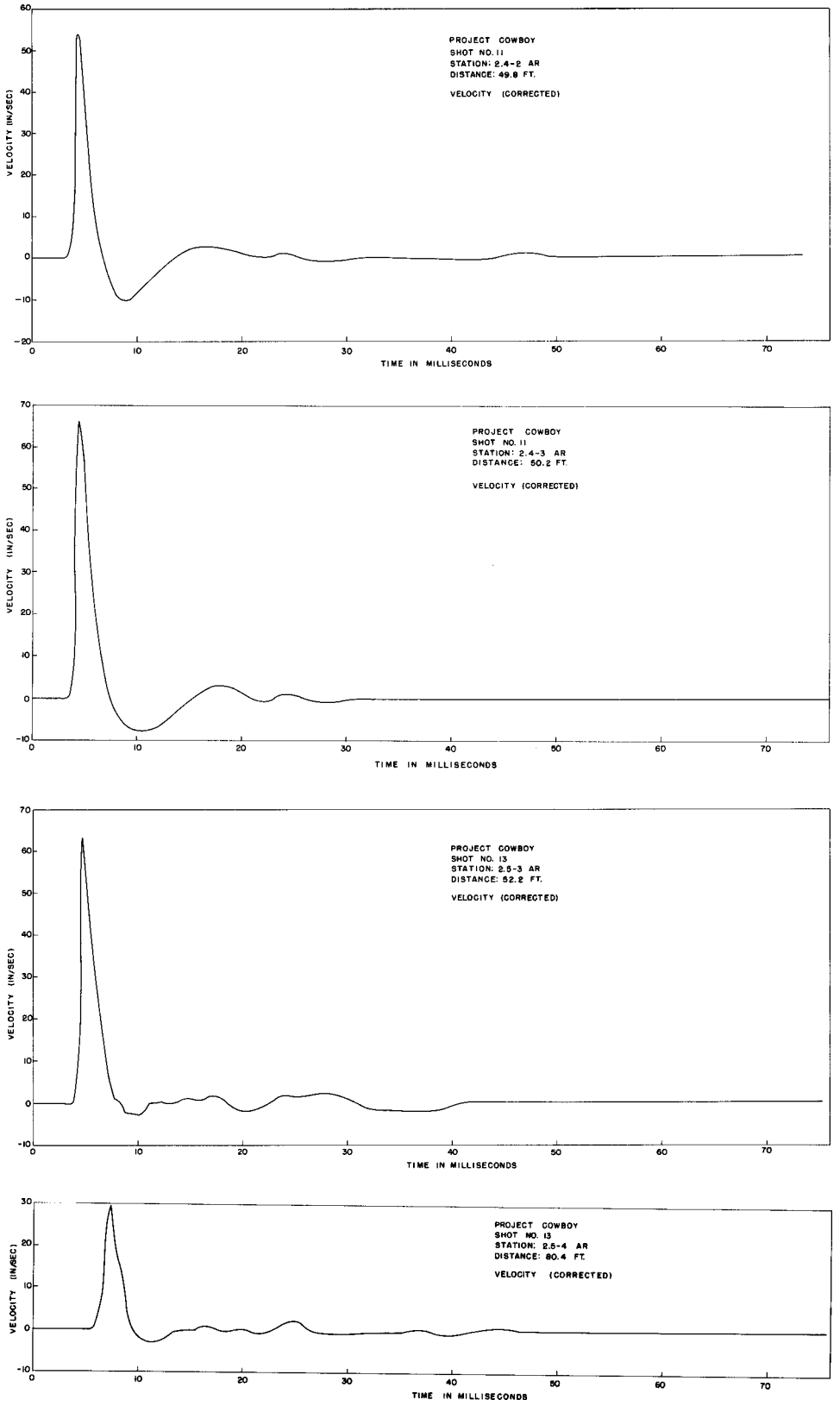

Fig. 3.32 Velocity versus time from integration of acceleration recordings

Corresponding displacements from integration of velocity-time data are shown in Fig. 3.33. Uncertainty in the accuracy of these integrations is illustrated by comparing the result for gage 2.5-4-AR at 80.9 feet with the result obtained from velocity gage 2.5-4-V located at the same position. Integration of acceleration gives a permanent displacement of 38 mils, whereas velocity integration gives 8 mils (Fig. 3.28). Clearly little reliance can be placed on numbers obtained for permanent displacement. On the other hand, peak displacements are quite reliable since they occur at an early enough time for the cumulative error to be small.

3.8 CAVITY WALL STRAINS

The attempt to measure tangential strain of the cavity wall on Shot No. 10 was partially successful. Considerable high-frequency noise, presumably electrical pickup, obscured the measurement. However, the low-frequency components of the record of periods comparable to those recorded by velocity gages indicated peak strains near 50 to 60 microinches per inch. If peak displacement data are extrapolated to the cavity wall, similar peak strain is computed. (See Section 4.3.3.)

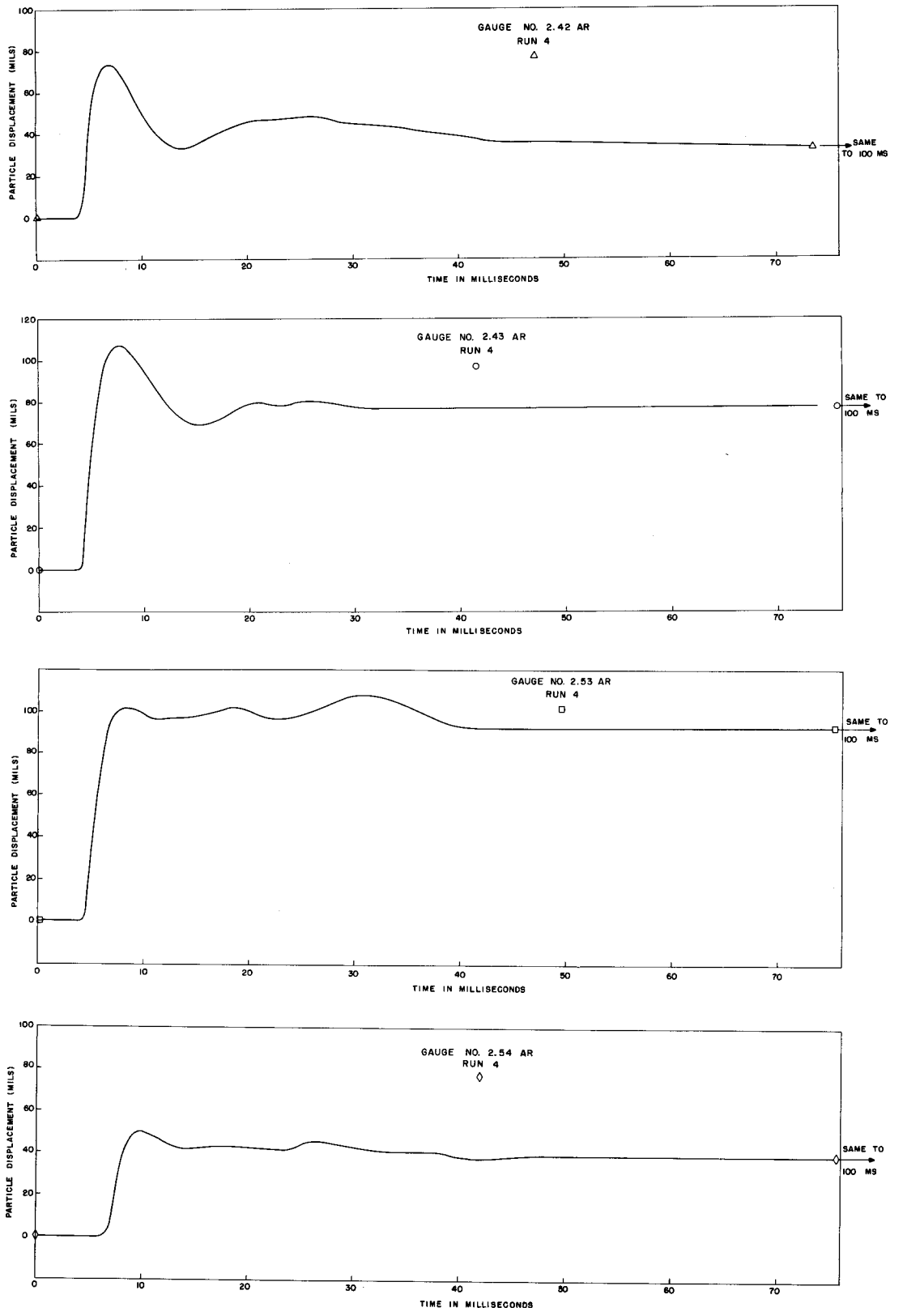

Fig. 3.33 Displacement versus time from double integration of acceleration recordings

Chapter 4

ANALYSIS OF RESULTS

4.1 DATA FROM PEAK VELOCITIES AND DISPLACEMENTS

Given observed data for tamped HE explosions in halite and theoretical behavior of a cavity, a decoupling factor can be calculated. This calculation will be compared with data obtained from the cavity explosions.

Consider the peak velocity and displacement plots for tamped explosions in Figs. 3.15 and 3.16. An effective elastic radius can be computed as a function of distance from the expression:

$$a_t = c \frac{d \text{ peak}}{u \text{ peak}} \quad ;$$

c is observed to be about 14,500 ft/sec from transit time between gage positions. The calculation gives, for 1000 pounds:

Distance of observation	a_t
1000 feet	22.8 feet
50 feet	16 feet

The variation reflects variation of d/u with distance. Presumably the ratio will not continue to change much more with distance, although complete changeover to 1/r behavior is not yet evident at 1000 feet. At scaled distances $r/W^{1/3} = 100$, the value of a will be $\sim 2.3\ W^{1/3}$ for explosions of Pelletol in halite. If the approximation that $c/a_t = 2\pi f$ is valid, the observed positive phase duration T of the velocity pulse should approximately equal 1/2f or $\pi a_t/c$. Since $\pi a_t/c$ = 5 milliseconds and T = 3-4 milliseconds, it is unlikely that a is much larger than 23 feet for 1000 pounds of Pelletol in halite. However, assumptions of elastic behavior beyond the "elastic radius" a_t are not entirely correct, since a_t depends upon the distance of observation.

The effective value of p_o at a_t can be calculated from

$$u = \frac{p_o}{\rho c} \frac{a_t}{r} \quad .$$

Taking r = 1000 feet

$u = 0.59$ in/sec = 1.5 cm/sec

$a_t = 23$ feet

$\rho = 2.13$ gm/cc

$c = 14{,}500$ ft/sec = 4.4×10^5 cm/sec

then $p_o = 61$ bars = 900 psi $\cong$ 1000 psi

Provided the cavity can withstand 1000 psi and an explosion yield is chosen to give 1000 psi in the cavity, the theoretical distant decoupling factor is simply a_t^3/a^3 where a_t is the tamped elastic radius and a is the cavity radius. Using Eq. 1.2, the value of W required to give 1000 psi in a 15-foot cavity is 6900 pounds. The corresponding a_t = 44 feet. This "theoretical" distant decoupling factor, a_t^3/a^3 is 25 for halite. Comparison with close-in observation follows.

Observed decoupling factors for peak velocities and displacements permit calculation of distance decoupling factors for each halite experiment. From Eqs. 1.9, 1.10, and 1.11, the distant decoupling factor is just

$$\left(\frac{d_t}{d_c}\right)^2 \Big/ \frac{u_t}{u_c} \quad .$$

Results in the following table yield numbers as much as 4 to 5 times larger than the number calculated above.

The third column gives distant decoupling factors which would be observed by distant velocity or displacement meters responsive at low frequencies. The numbers apply only to the specific experiment to which

TABLE 4.1--DECOUPLING FACTORS - HE IN HALITE
(from peak values)

$\frac{u_t}{u_c}$	$\frac{d_t}{d_c}$	$\left(\frac{d_t}{d_c}\right)^2 \Big/ \frac{u_t}{u_c}$	W (lbs)	r (feet)	Shot No. (cavity)	Cavity Radius (feet)
20	30.5	47	200	200	6	15
7.3	23	72	500	370	8	15
7.5	30	120	1000	365	10	15
35	--	--	20	35	2	6
25	--	--	100	35	3	6
6.7	10	15	1000	460	12	6
5	8.6	15	2000	460	14	6

they refer, i.e., tamped and cavity HE explosions in halite. Smaller numbers could easily be observed in the Cowboy experiments by nearby surface instruments of proper frequency response.

The numbers listed in column 3, Table 4.1, are not precise, since the condition that the comparison be made in the region where velocities fall off inversely as distance is not fulfilled. Table 4.2 shows how the numbers vary with distance of comparison.

TABLE 4.2--DECOUPLING VERSUS DISTANCE OF CLOSE-IN OBSERVATION

$\frac{u_t}{u_c}$	$\frac{d_t}{d_c}$	$\left(\frac{d_t}{d_c}\right)^2 \Big/ \frac{u_t}{u_c}$	r (feet)	Shot No.
15	39.2	100	50	8
13.9	43.8	138	80	8
9.3	29	91	200	8
7.3	23	72	370	8

The reason the decoupling factor is higher for the higher yield explosions in the 15-foot cavity is simply that the recorded pulse from the cavity

is relatively sharper for the higher yield explosions. The duration of the velocity pulse from the tamped explosion increases with yield as $W^{1/3}$. Velocity pulses for the cavity retained a higher frequency content than would be characteristic of the oscillating cavity and are really more characteristic of the driving pressure pulses.

The reason that the observed distant decoupling factors are nearer 100 than 25 appears to be that more of the energy is concentrated in high frequencies than is allowed for in the calculation. The afterpressure at 100 milliseconds is also smaller than calculated from Eq. 1.2. Experimentally, the afterpressure at 100 milliseconds from 1000 pounds in the 15-foot cavity was 92 psi. According to this observation, 11,000 pounds of Pelletol would be required to give 1000 psi at 100 milliseconds after the explosion. On this basis, a_t for 11,000 pounds is 51 and a_t^3/a^3 would be 40. Since the effective value of a_t calculated from distant observations would be larger than used here, distant decoupling factors between 40 and 100 can be estimated from the close-in observed peak velocities and displacements for these particular Cowboy experiments in the 15-foot cavity.

The same calculation made for the 15-foot cavity above can be made for the 6-foot cavity and should give the same result. The filling weight to give 1000 psi is 710 pounds, for which a_t = 20.6 feet and a_t^3/a^3 = 40.

4.2 DATA FROM PERMANENT DISPLACEMENT FROM LOW-PASS ACCELEROMETER OBSERVATIONS

A low-frequency displacement amplitude of about 0.012 inch was observed at 80.9 feet from 1000-pound coupled Shot No. 13. Equation 1.1 may be used to calculate the distant decoupling in halite:

$$\text{Decoupling factor} = \frac{16\pi}{3(\gamma - 1)} \mu_h \frac{r_o^2 d_o}{W}$$

where $\gamma = 1.2$

$\mu_h = 100$ kilobars $= 100 \times 10^9$ dynes/cm^2

$W = 1.9 \times 10^{16}$ ergs

$c_h = c$

Decoupling factor = 80.

Two possible difficulties arise in connection with the above calculation: (1) Possibly the small permanent displacements of 1 to 10 mils are somehow obscured by instrument placement, and (2) the idea that $r_o^2 d_o$ is still constant out to $r/W^{1/3} = 8$ is not necessarily valid. The medium is elastic at this distance, and a very small void ratio would allow rebound to obscure the permanent displacement observable at $r/W^{1/3} = 2$ to 3. Permanent displacement measurements must be made very near the elastic radius to overcome both difficulties mentioned above.

4.3 ELASTIC CAVITY BEHAVIOR

4.3.1 Velocity and Earth Pressure

If velocity and pressure peaks are truly related by $p = \rho cu$ in the region of observation, then p at the wall may be calculable by extrapolation of u to the wall. Using $\rho = 2.13$ g/cc and $c = 14{,}500$ ft/sec:

Shot No. (cavity)	W (lbs)	p(observed) (psi)	u (in/sec)	p(from 35 ρcu) (psi)
5,6	200	~300	4	140
8	500	500	14.5	510
10	1000	900	25	870

The agreement on Shots 8 and 10 is as good as the accuracy of the instrumentation. In all cases, the velocity gage was barely capable of following the pressure pulse; the limitation is most severe on Shots 5 and 6.

Earth pressure gages, placed at 50 feet radius from the 15-foot cavity, produced records very similar in appearance to velocity records at the same positions (Figs. 4.1 and 4.2). The piezoelectric elements of these earth pressure gages were oil-coupled and hence, nondirectional. Exact calibration is still in doubt. If the most appropriate calibration is used, results for Shot 10 are:

Distance (feet)	Peak earth pressure (psi)	Peak velocity (in/sec)	$p = \rho cu$ (psi)
23.9	370	13	450
49.9	240	5.1	180
50.5	180	6	210

4.3.2 Natural Period of Cavity

The natural period of oscillation of the 15-foot cavity calculated from $\frac{T}{2\pi} = \frac{a}{c}$ is 6.5 msec. (Correction for $\sigma = 0.3$ gives a longer period; $\frac{T}{2\pi} = \frac{a}{c}\frac{(1-\sigma)}{\sqrt{1-2\sigma}} = 1.1 \times 6.5 = 7.16$ msec.)

Cavity oscillation does not show up in the velocity records, since peak velocities are so high compared to velocities from the ringing cavity. Numerous oscillating gas-pressure pulses are clearly recorded by velocity gages. Integrated velocity records provide some measure of cavity oscillation. Experimental displacement gage records give excellent signal-to-noise ratio for transient displacement and clearly show cavity oscillation (Figs. 4.3 and 4.4). Periods of successive cycles range from 5.5 to 7 milliseconds, bracketing the theoretical value, $\frac{2\pi a}{c}$. Note that the cavity seems to be more highly damped for the 1000-pound shot than for the 500-pound shot.

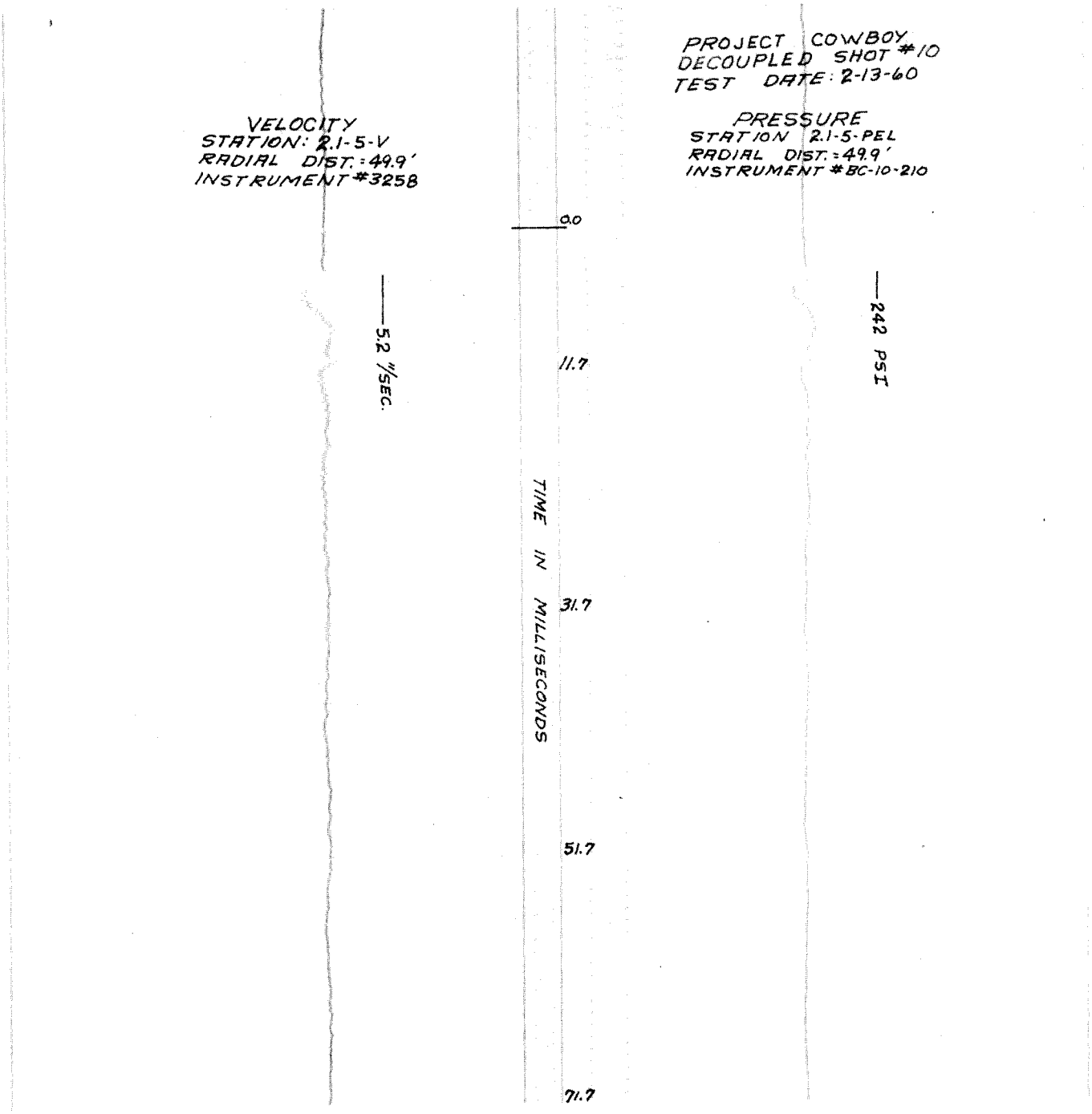

Fig. 4.1 Particle velocity and earth pressure versus time

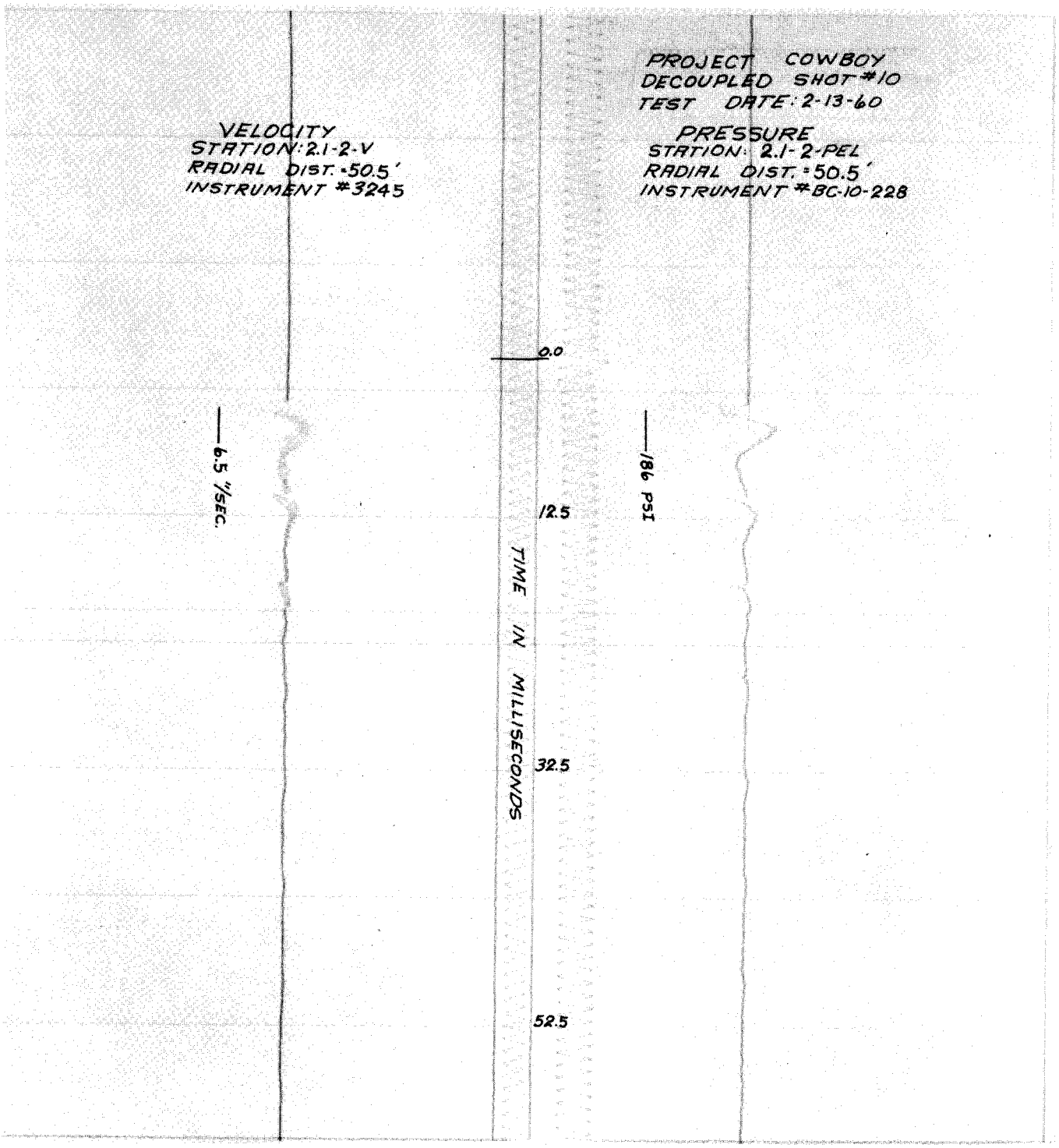

Fig. 4.2 Particle velocity and earth pressure versus time

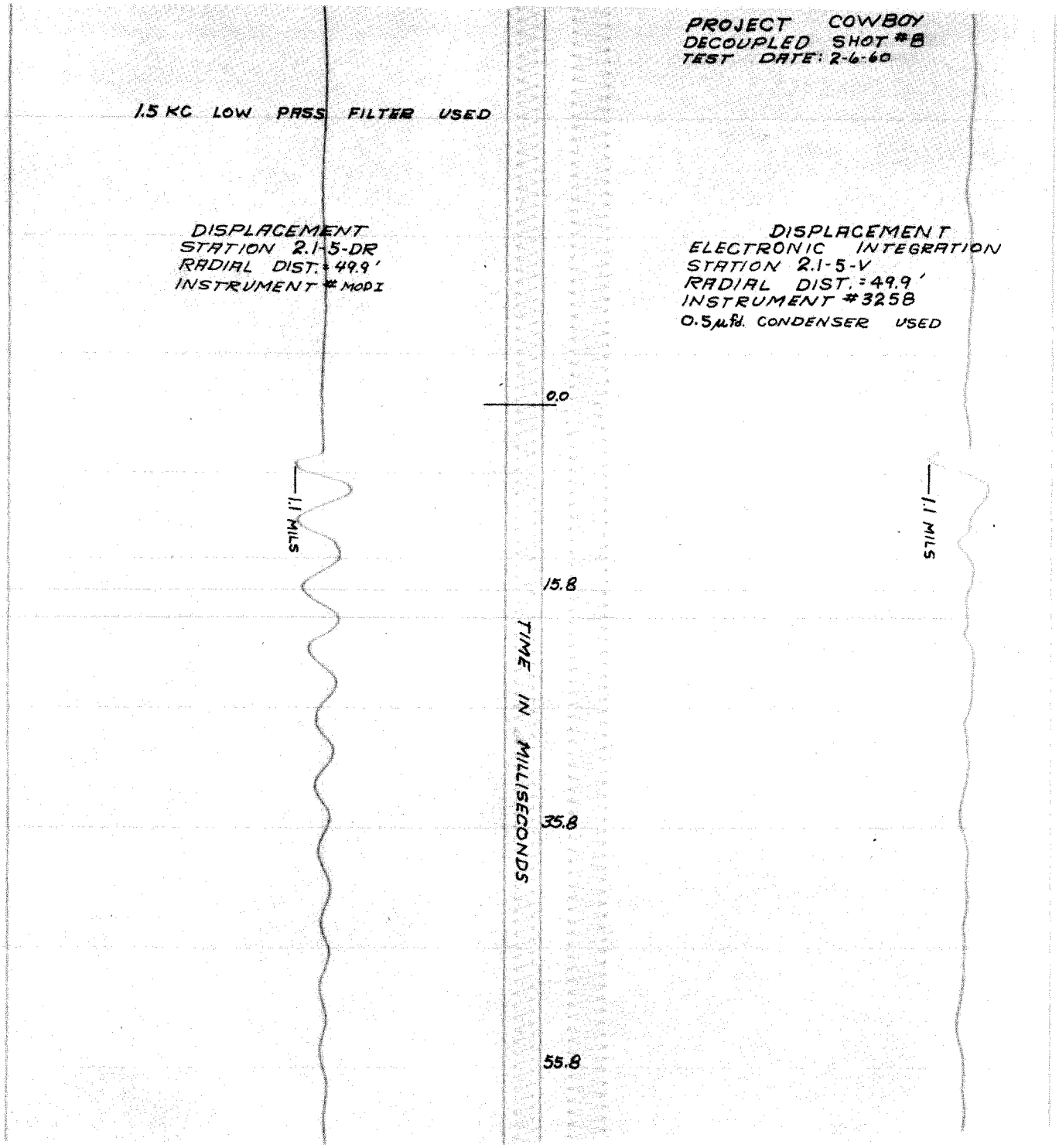

Fig. 4.3 Displacement and integrated velocity versus time

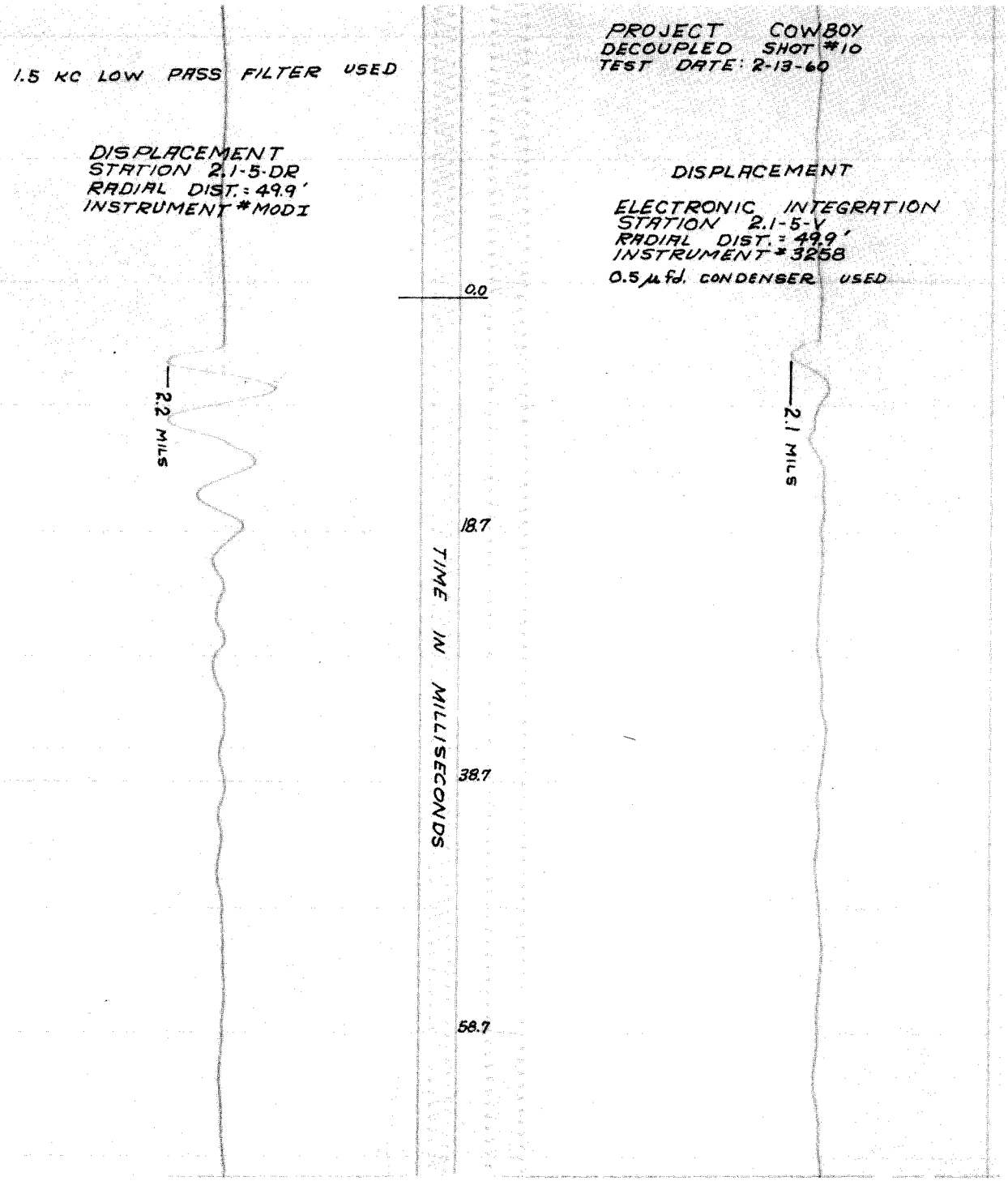

Fig. 4.4 Displacement and integrated velocity versus time

4.3.3 Tensile Failure

Extrapolation of peak velocities and displacements in Figs. 3.7 and 3.8 to the 6-foot cavity wall gives peak velocity = 130 in/sec and peak displacement = 100 mils. The corresponding peak radial-compressive strain and peak tangential-tensile strain are, therefore, for 929 pounds of Pelletol:

$$E_r = \frac{u}{c} = 750\ \mu\text{in/in} \qquad \text{compression}$$

$$E_t = \frac{d}{r} = 1400\ \mu\text{in/in} \qquad \text{tension}$$

Similarly, for 1900 pounds in the 6-foot-radius cavity:

$$E_r = 1800\ \mu\text{in/in} \qquad \text{compression}$$

$$E_t = 4200\ \mu\text{in/in} \qquad \text{tension}$$

Unconfined halite specimens in laboratory tests exhibit a Young's modulus near 800,000 psi and tensile failure at less than 100 psi. Tensile strength of the cavity wall is almost entirely due to overburden compressive stress to be overcome before the wall goes into tension. Since large tensile strains occurred, the wall developed tensile cracks. Compressive strains were too small to result in failure in compression, as several thousand μin/in would be required.

At the time of maximum tangential-tensile strain, the radial strain is zero. Shortly afterwards small tensile radial strain develops, so that some spalling would occur if a large enough shot were fired in the cavity. As yield increases from small values, radial cracking extends further and further from the wall, causing the cavity behavior to be inelastic. Apparently serious cracking does not occur until the confining overburden pressure is considerably exceeded.

4.3.4 Elastic Constants

Propagation velocities in the halite were observed to be 14,500 to 15,000 ft/sec from transit time between velocity gages. In this report we have used c = 14,500 ft/sec for halite and ρ = 2.13 g/cc. With these numbers,

$$\lambda + 2\mu = 415 \text{ kilobars}$$

If $\lambda = \mu$, $\sigma = 0.25$, $\mu = 137$ kilobars

If $\lambda = 2\mu$, $\sigma = 0.3$, $\mu = 103$ kilobars

Shear-wave velocity was not determined from our records, since gages were always radial except for the distant accelerometers where reflections obscure the data.

Chapter 5

CONCLUSIONS AND RECOMMENDATIONS

5.1 CONCLUSIONS

Radial motion close to tamped explosions in halite was adequately determined over scaled distances from 6 ft/lb$^{1/3}$ to 80 ft/lb$^{1/3}$. Permanent displacements at the closest ranges were less than would be expected for incompressible motion. Evidently measurements as close as a scaled distance of 2 ft/lb$^{1/3}$ are needed to obtain an accurate measure of permanent displacement from tamped explosions. It is suggested that for 1000-pound explosions measurements be obtained at distances of 20, 30, and 50 feet, but it should be noted that accelerometers or long-base displacement gages would have to be used. Larger explosions would make measurements easier to obtain. Pressure measurements should also be made in the halite at the same distances as a check on the degree of elastic behavior.

Adequate measure of motion near the cavities is difficult to obtain because the centrally located charge gives a fast-rising, short-duration pulse that is difficult to measure unless the HE charges are large. Measurements for 500-pound-and-larger charges appear to be good enough. Low-frequency motions near the cavities were too small for us to measure. Use of gas in the cavities would presumably make the fast pressure pulse less significant and make measurement easier. The experimental displacement gage is useful down to 10 cps, but not useful for permanent displacement; some other scheme should be added. We suggest that long-base strain gages may prove satisfactory. Permanent displacement is naturally easier to measure when such large charges are fired that the cavity wall deforms plastically. As this

condition is approached, the long-base strain (relative displacement) gage[5] will give useful results.

Enough transient measurements were obtained to make possible a calculation of the motion near the 15-foot cavity. Such calculations need only use the observed pressure-time history on the wall as an input to equations described by Sharpe[2] or Blake.[6] Computed transient velocities may then be compared with observations of velocity versus time. Such calculations will be published separately. Clearly, motion of the medium near the cavity depends on details of the pressure-time history in the cavity. Empirically, motion at large distances from the cavity falls off faster than inversely as the distance. If this is due to attenuation of high frequencies caused by frictional effects, then it would not occur to the same extent for larger cavities and larger explosions. Scaling of these data to very large HE explosions is not necessarily accurate.

Data obtained on Cowboy definitely proves that decoupling of the distant signal in halite of a factor from 40 to 100 can be obtained for high explosives. Quantitative evaluation of the degree of decoupling that could be obtained from nuclear explosions can only be obtained from nuclear explosions for two reasons: (1) A tamped nuclear explosion starts off at many times higher pressure in the medium. In fact, the starting pressure increases with nuclear yield, so that nuclear explosions of different yield do not even exhibit similar behavior. Thus, the similarity principle invoked for various yield HE explosions cannot be used in the same way for nuclear explosions. (2) A nuclear explosion in a cavity will behave in a manner different from an explosion of HE simply because of the very different pressure time history of the nuclear explosion.

5.2 RECOMMENDATIONS

Decoupling factors for nuclear explosions should be obtained by detonation of charges with yields as large as might be decoupled in a practical manner. Cowboy experiments prove that explosions can be muffled, but the exact decoupling that can be obtained from a practical cavity can only be determined by detonation of a nuclear explosion (see end of Section 5.2).

Close-in measurements of displacement should be obtained by means of long-base strain gages. Displacement measurements should be made as near the explosion as reliable operation of gages permits.

Stress measurements in rock should be made to check on the degree of elastic behavior.

The appropriate type of gage to be used depends on the size of explosion. Accelerometers can always be used, but it is desirable to employ velocity and relative-displacement gages if appropriate designs can be evolved.

REFERENCES

1. Latter, A. L., LeLevier, R. E., Martinelli, E. A., and McMillan, W. G., "A Method of Concealing Underground Nuclear Explosions," R-348, RAND Corporation, 1959.

2. Sharpe, J. A., "The Propagation of Elastic Waves by Explosive Pressures," Geophysics, Vol. 7, 1942, pp. 144-154, 311-321.

3. Cole, R. H., "Underwater Explosions," Princeton University Press, 1948.

4. Nuckolls, John, Unpublished Notes.

5. Perret, W. R., "Ground Motion Studies at High Incident Overpressure," WT-1405, Sandia Corporation, 1960.

6. Blake, F. G., Jr., "Spherical Wave Propagation in Solid Media," Journal of the Acoustical Society of America 24, 1952, pp. 211-215.

DISTRIBUTION

No. of Copies	Addressee
1	E. N. Parker, HQ/DASA
1	A. D. Starbird, DMA, AEC
10	I. Maddock, OBE, AWRE, thru DMA
1	W. S. Long, BJSM, thru DMA
1	W. J. Manning, DMA, AEC
5	Department of State, thru DMA
2	G. B. Kistiakowsky, thru DMA
10	J. Rosen, DMA, AEC
1	C. H. Reichardt, Div. of Intelligence, AEC, Washington, D. C.
5	C. F. Romney, thru DMA
25	J. G. Lewis, HQ/DASA
5	I. D. Brent, II, thru DMA
3	J. R. Balsley, U. S. Geological Survey, Washington, D. C.
3	D. S. Carder, U. S. Coast and Geodetic Survey, Washington, D.C.
5	J. E. Crawford, Bureau of Mines, Washington, D. C.
20	J. E. Reeves, OTO, ALO
3	L. S. Ayers, SAN
3	W. K. Cloud, U. S. Coast and Geodetic Survey, San Francisco
2	R. B. Vaile, Jr., Stanford Research Institute, Menlo Park, Calif.
2	R. M. Foose, Stanford Research Institute, Menlo Park, Calif.
2	T. C. Poulter, Stanford Research Institute, Menlo Park, Calif.
5	N. E. Bradbury, LASL
1	F. Press, Calif. Institute of Technology, Pasadena
1	H. Benioff, Calif. Institute of Technology, Pasadena
1	J. E. Oliver, Columbia University New York
4	W. G. McMillan, RAND Corp., Santa Monica, Calif.
1	H. A. Bethe, Cornell University Ithaca, New York
1	S. B. Smith, Holmes and Narver, Los Angeles, Calif.
1	H. E. Grier, EG&G, Las Vegas
1	F. B. Porzel, Armour Research Foundation, Chicago, Ill.
1	W. B. Heroy, Sr., The Geotechnical Corp., Dallas, Texas
2	L. Strickland, Texas Instruments, Inc., Dallas, Texas
1	W. R. Mitchell, National Geophysical Corp., Dallas, Texas
1	J. T. Wilson, University of Michigan
1	R. F. Hautley, Sprengnether Instrument Co., St. Louis, Mo.
1	D. N. Tocher, University of Calif., Berkeley, Calif.
1	P. D. Trask, University of Calif., Berkeley, Calif.
1	B. Sussholz, STL, Inglewood, Calif.
50	A. V. Shelton, Jr., LRL
1	J. P. Molnar, 1
1	G. A. Fowler, 5000
1	C. F. Quate, 5100
1	T. B. Cook, Jr., 5110
10	B. F. Murphey, 5112
1	W. W. Bledsoe, 5120
1	M. L. Merritt, 5130
1	A. Y. Pope, 5140
1	R. S. Claassen, 5150
1	D. B. Shuster, 5200
1	H. H. Patterson, 5230
1	H. E. Hansen, 5251
1	A. D. Thornbrough, 5251-1
1	R. J. Tockey, 8123
1	R. E. Dewhurst, 8233
1	R. K. Smeltzer, 3421-3
1	W. F. Carstens, 3423
5	Mrs. W. K. Cox, 3466-1
216	

TITLES OF REPORTS ISSUED BY AGENCIES PARTICIPATING IN PROJECT COWBOY

Agency	Title	Author
SC, Abq	Particle Motions near Explosions in Halite	B. F. Murphey
USC&GS	Seismic Ground Effects from Coupled and Decoupled Shots in Salt	D. S. Carder, et al.
APRL	1. Dynamic Strain Measurements in Salt - Part I 2. Dynamic Strain Measurements in Salt - Part II 3. Static Stress Measurements in Salt	L. A. Obert and/or Associates
BuMines, Pit	Investigations Relating to Gas-Phase Detonations	R. W. VanDolah and/or Associates
WES	Drilling and Grouting Support	J. M. Polatty
SRI	Investigations of On-Site Inspection Techniques for High-Explosive Tests in a Salt Mine	R. B. Hoy and Associates
SC, Livermore	High Explosives - Arming and Firing	R. J. Tockey and Associates
LRL	Seismic Decoupling in Spherical Cavities	W. M. Adams and D. S. Carder
LRL	Permanent Deformation	W. A. Hamilton et al.
LRL	Close-In Pressure Measurements with Tourmaline Crystals on Tamped Detonations	W. F. Lindsay et al.
EG&G Boston	Timing and Firing of High Explosives	S. R. Hamilton et al.
LRL	Instrument Chart and Miscellaneous Engineering Information	R. B. Petrie et al.
LRL	Interpretation of the Seismic Data	R. F. Herbst and G. C. Werth
LRL	Analysis and Interpretation of Close-In Measurements	J. H. Nuckolls
LRL	Physical Properties of Salt Samples	S. E. Warner et al.